

E.; Gargiulo, C.; Gasik, P.; Gaur, H. m.; Gautam, A.; Gay Ducati, M. b.; Germain, M.; Ghosh, C.; Giacalone, M.; Gioachin, G.; Giubellino, P.; Giubilato, P.; Glaenger, A. m. c.; Glässel, P.; Glimos, E.; Goh, D. j. q.; Gonzalez, V.; Gordeev, P.; Gorgon, M.; Goswami, K.; Gotovac, S.; Grabski, V.; Graczykowski, L. k.; Grecka, E.; Grelli, A.; Grigoras, C.; Grigoriev, V.; Grigoryan, S.; Grosa, F.; Grosse-Oetringhaus, J. f.; Grosso, R.; Grund, D.; Grunwald, N. a.; Guardiano, G. g.; Guernane, R.; Guillbaud, M.; Gulbrandsen, K.; Gumprecht, J. j. w. k.; Gündem, T.; Gunji, T.; Guo, W.; Gupta, A.; Gupta, R.; Gupta, R.; Gwizdziel, K.; Gyulai, L.; Hadjidakis, C.; Haider, F. u.; Haidlova, S.; Haldar, M.; Hamagaki, H.; Hamdi, A.; Han, Y.; Hanley, B. g.; Hannigan, R.; Hansen, J.; Haque, M. r.; Harris, J. w.; Harton, A.; Hartung, M. v.; Hassan, H.; Hatzifotiadou, D.; Hauer, P.; Havener, L. b.; Hellbär, E.; Helstrup, H.; Hemmer, M.; Herman, T.; Hernandez, S. g.; Herrera Corral, G.; Herrmann, S.; Hetland, K. f.; Heybeck, B.; Hillemanns, H.; Hippolyte, B.; Hoffmann, F. w.; Hofman, B.; Hong, G. h.; Horst, M.; Horzyk, A.; Hou, Y.; Hristov, P.; Huhn, P.; Huhta, L. m.; Humanic, T. j.; Hutson, A.; Hutter, D.; Hwang, M. c.; Ilkaev, R.; Inaba, M.; Innocenti, G. m.; Ippolitov, M.; Isakov, A.; Isidori, T.; Islam, M. s.; Iurchenko, S.; Ivanov, M.; Ivanov, M.; Ivanov, V.; Iversen, K. e.; Jablonski, M.; Jacak, B.; Jacazio, N.; Jacobs, P. m.; Jadlovská, S.; Jadlovsky, J.; Jaelani, S.; Jahnke, C.; Jakubowska, M. j.; Janik, M. a.; Janson, T.; Ji, S.; Jia, S.; Jimenez, A. a. p.; Jonas, F.; Jones, D. m.; Jowett, J. m.; Jung, J.; Jung, M.; Junique, A.; Jusko, A.; Kaewjai, J.; Kalinak, P.; Kalweit, A.; Karasu Uysal, A.; Karatovic, D.; Karatzenis, N.; Karavichev, O.; Karavicheva, T.; Karpechev, E.; Karwowska, M. j.; Kebschull, U.; Keidel, R.; Keil, M.; Ketzer, B.; Khade, S. s.; Khan, A. m.; Khan, S.; Khanzadeev, A.; Kharlov, Y.; Khatun, A.; Khuntia, A.; Khuranova, Z.; Kileng, B.; Kim, B.; Kim, C.; Kim, D. j.; Kim, E. j.; Kim, J.; Kim, J.; Kim, J.; Kim, M.; Kim, S.; Kim, T.; Kimura, K.; Kirkova, A.; Kirsch, S.; Kisel, I.; Kiselev, S.; Kisiel, A.; Kitowski, J. p.; Klay, J. I.; Klein, J.; Klein, S.; Klein-Bösing, C.; Kleiner, M.; Klemenz, T.; Kluge, A.; Kobdaj, C.; Kohara, R.; Kollegger, T.; Kondratyev, A.; Kondratyeva, N.; König, J.; Königstorfer, S. a.; Konopka, P. j.; Kornakov, G.; Korwieser, M.; Koryciak, S. d.; Koster, C.; Kotliarov, A.; Kovacic, N.; Kovalenko, V.; Kowalski, M.; Kozuharov, V.; Králik, I.; Kraváková, A.; Krcal, L.; Krivda, M.; Krizek, F.; Krizkova Gajdosova, K.; Krug, C.; Krüger, M.; Krupova, D. m.; Kryshen, E.; Kuera, V.; Kuhn, C.; Kuijjer, P. g.; Kumaoka, T.; Kumar, D.; Kumar, L.; Kumar, N.; Kumar, S.; Kundu, S.; Kurashvili, P.; Kurepin, A.; Kurepin, A. b.; Kuryakin, A.; Kushpil, S.; Kuskov, V.; Kutyla, M.; Kweon, M. j.; Kwon, Y.; La Pointe, S. I.; La Rocca, P.; Lakrathok, A.; Lamanna, M.; Landou, A. r.; Langoy, R.; Larionov, P.; Laudi, E.; Lautner, L.; Laveaga, R. a. n.; Lavicka, R.; Lea, R.; Lee, H.; Legrand, I.; Legras, G.; Lehrbach, J.; Lelek, T. m.; Lemmon, R. c.; León Monzón, I.; Lesch, M. m.; Lesser, E. d.; Lévai, P.; Li, M.; Li, X.; Liang-gilman, B. e.; Lien, J.; Lietava, R.; Likmeta, I.; Lim, B.; Lim, S. h.; Lindenstruth, V.; Lindner, A.; Lippmann, C.; Liu, D. h.; Liu, J.; Liveraro, G. s. s.; Lofnes, I. m.; Loizides, C.; Lokos, S.; Lömker, J.; Lopez, X.; López Torres, E.; Lu, P.; Lugo, F. v.; Luhder, J. r.; Lunardon, M.; Luparello, G.; Ma, Y. g.; Mager, M.; Maire, A.; Majerz, E. m.; Makariev, M. v.; Malaev, M.; Malfattore, G.; Malik, N. m.; Malik, Q. w.; Malik, S. k.; Malinina, L.; Mallick, D.; Mallick, N.; Mandaglio, G.; Mandal, S. k.; Manea, A.; Manko, V.; Manso, F.; Manzari, V.; Mao, Y.; Marcjan, R. w.; Margagliotti, G. v.; Margotti, A.; Marín, A.; Markert, C.; Martinengo, P.; Martínez, M. i.; Martínez García, G.; Martins, M. p. p.; Masciocchi, S.; Maserà, M.; Masoni, A.; Massacrier, L.; Massen, O.; Mastroserio, A.; Matonoha, O.; Mattiazzo, S.; Matyja, A.; Mazuecos, A. I.; Mazzaschi, F.; Mazzilli, M.; Mdhluli, J. e.; Melikyan, Y.; Menchaca-Rocha, A.; Mendez, J. e. m.; Meninno, E.; Menon, A. s.; Menzel, M. w.; Meres, M.; Miake, Y.; Micheletti, L.; Mihaylov, D. I.; Mikhaylov, K.; Minafra, N.; Mikowiec, D.; Modak, A.; Mohanty, B.; Khan, M. Mohisin; Molander, M. a.; Monira, S.; Mordasini, C.; Moreira De Godoy, D. a.; Morozov, I.; Morsch, A.; Mrnjavac, T.; Muccifora, V.; Muhuri, S.; Mulligan, J. d.; Mulliri, A.; Munhoz, M. g.; Munzer, R. h.; Murakami, H.; Murray, S.; Musa, L.; Musinsky, J.; Myrcha, J. w.; Naik, B.; Nambrath, A. i.; Nandi, B. k.; Nania, R.; Nappi, E.; Nassirpour, A. f.; Nath, A.; Natrass, C.; Naydenov, M. n.; Neagu, A.; Negro, A.; Nekrasova, E.; Nellen, L.; Nepeivoda, R.; Nese, S.; Neskovic, G.; Nicassio, N.; Nielsen, B. s.; Nielsen, E. g.; Nikolaev, S.; Nikulin, S.; Nikulin, V.; Noferini, F.; Noh, S.; Nomokonov, P.; Norman, J.; Novitzky, N.; Nowakowski, P.; Nyanin, A.; Nystrand, J.; Oh, S.; Ohlson, A.; Okorokov, V. a.; Oleniacz, J.; Onnerstad, A.; Oppedisano, C.; Ortiz Velasquez, A.; Otwinowski, J.; Oya, M.; Oyama, K.; Pachmayer, Y.; Padhan, S.; Pagano, D.; Pai, G.; Paisano-Guzmán, S.; Palasciano, A.; Panebianco, S.; Park, H.; Park, H.; Park, J.; Parkkila, J. e.; Patley, Y.; Paul, B.; Paulino, M. m. d. m.; Pei, H.; Peitzmann, T.; Peng, X.; Pennisi, M.; Perciballi, S.; Peresunko, D.; Perez, G. m.; Pestov, Y.; Petersen, M. t.; Petrov, V.; Petrovici, M.; Piano, S.; Pikna, M.; Pillot, P.; Pinazza, O.; Pinsky, L.; Pinto, C.; Pisano, S.; Posko, M.; Planinic, M.; Pliquett, F.; Poghosyan, M. g.; Polichtchouk, B.; Politano, S.; Poljak, N.; Pop, A.; Porteboeuf-Houssais, S.; Pozdniakov, V.; Pozos, I. y.; Pradhan, K. k.; Prasad, S. k.; Prasad, S.; Preghenella, R.; Prino, F.; Pruneau, C. a.; Pshenichnov, I.; Puccio, M.; Pucillo, S.; Qiu, S.; Quaglia, L.; Ragoni, S.; Rai, A.; Rakotozafindrabe, A.; Ramello, L.; Rami, F.; Rasa, M.; Räsänen, S. s.; Rath, R.; Rauch, M. p.; Ravasenga, I.; Read, K. f.; Reckziegel, C.; Redelbach, A. r.; Redlich, K.; Reetz, C. a.; Regules-Medel, H. d.; Rehman, A.; Reidt, F.; Reme-Ness, H. a.; Rescakova, Z.; Reygers, K.; Riabov, A.; Riabov, V.; Ricci, R.; Richter, M.; Riedel, A. a.; Riegler, W.; Riffero, A. g.; Ripoli, C.; Ristea, C.; Rodriguez, M. v.; Rodríguez Cahuantzi, M.; Rodríguez Ramírez, S. a.; Røed, K.; Rogalev, R.; Rogochaya, E.; Rogoschinski, T. s.; Rohr, D.; Röhrich, D.; Rojas Torres, S.; Rokita, P. s.; Romanenko, G.; Ronchetti, F.; Rosas, E. d.; Roslon, K.; Rossi, A.; Roy, A.; Roy, S.; Rubini, N.; Rudolph, J. a.; Ruggiano, D.; Rui, R.; Russek, P. g.; Russo, R.; Rustamov, A.; Ryabinkin, E.; Ryabov, Y.; Rybicki, A.; Ryu, J.; Rzesza, W.; Sadhu, S.; Sadovsky, S.; Saetre, J.; Šafaik, K.; Saha, S. k.; Saha, S.; Sahoo, B.; Sahoo, R.; Sahoo, S.; Sahu, D.; Sahu, P. k.; Saini, J.; Sajdakova, K.; Sakai, S.; Salvan, M. p.; Sambyal, S.; Samitz, D.; Sanna, I.; Saramela, T. b.; Sarkar, D.; Sarma, P.; Sarritzu, V.; Sarti, V. m.; Sas, M. h. p.; Sawan, S.; Scapparone, E.; Schambach, J.; Scheid, H. s.; Schiaua, C.; Schicker, R.; Schlepper, F.; Schmah, A.; Schmidt, C.; Schmidt, H. r.; Schmidt, M. o.; Schmidt, M.; Schmidt, N. v.; Schmier, A. r.; Schotter, R.; Schröter, A.; Schukraft, J.; Schweda, K.; Scioli, G.; Scomparin, E.; Seger, J. e.; Sekiguchi, Y.; Sekihata, D.; Selina, M.; Selyuzhenkov, I.; Senyukov, S.; Seo, J. j.; Serebryakov, D.; Serkin,

L.; Šerkšnyt, L.; Sevcenco, A.; Shaba, T. j.; Shabetai, A.; Shahoyan, R.; Shangaraev, A.; Sharma, B.; Sharma, D.; Sharma, H.; Sharma, M.; Sharma, S.; Sharma, S.; Sharma, U.; Shatat, A.; Sheibani, O.; Shigaki, K.; Shimomura, M.; Shin, J.; Shirinkin, S.; Shou, Q.; Sibiriak, Y.; Siddhanta, S.; Siemiarczuk, T.; Silva, T. f.; Silvermyr, D.; Simantathammakul, T.; Simeonov, R.; Singh, B.; Singh, B.; Singh, K.; Singh, R.; Singh, R.; Singh, R.; Singh, S.; Singh, V. k.; Singhal, V.; Sinha, T.; Sitar, B.; Sitta, M.; Skaali, T. b.; Skorodumovs, G.; Smirnov, N.; Snellings, R. j. m.; Solheim, E. h.; Song, J.; Sonnabend, C.; Sonneveld, J. m.; Soramel, F.; Soto-hernandez, A. b.; Spijkers, R.; Sputowska, I.; Staa, J.; Stachel, J.; Stan, I.; Steffanic, P. j.; Stiefelmaier, S. f.; Stocco, D.; Storehaug, I.; Strangmann, N. j.; Stratmann, P.; Strazzi, S.; Sturniolo, A.; Stylianidis, C. p.; Suaide, A. a. p.; Suire, C.; Sukhanov, M.; Suljic, M.; Sultanov, R.; Sumberia, V.; Sumowidagdo, S.; Szarka, I.; Szymkowski, M.; Taghavi, S. f.; Taillepie, G.; Takahashi, J.; Tambave, G. j.; Tang, S.; Tang, Z.; Tapia Takaki, J. d.; Tapus, N.; Tarasovicova, L. a.; Tarzila, M. g.; Tassielli, G. f.; Tauro, A.; Tavira García, A.; Tejada Muñoz, G.; Telesca, A.; Terlizzi, L.; Terrevoli, C.; Thakur, S.; Thomas, D.; Tikhonov, A.; Tiltmann, N.; Timmins, A. r.; Tkacik, M.; Tkacik, T.; Toia, A.; Tokumoto, R.; Tomassini, S.; Tomohiro, K.; Topilskaya, N.; Toppi, M.; Tork, T.; Torres, V. v.; Torres Ramos, A. g.; Trifiró, A.; Triloki, T.; Triolo, A. s.; Tripathy, S.; Tripathy, T.; Trubnikov, V.; Trzaska, W. h.; Trzcinski, T. p.; Tsolanta, C.; Tumkin, A.; Turrisi, R.; Tveter, T. s.; Ullaland, K.; Ulukutlu, B.; Uras, A.; Urioni, M.; Usai, G. I.; Vala, M.; Valle, N.; Van Doremalen, L. v. r.; Van Leeuwen, M.; Van Veen, C. a.; Van Weelden, R. j. g.; Vande Vyvre, P.; Varga, D.; Varga, Z.; Vargas Torres, P.; Vasileiou, M.; Vasiliev, A.; Vázquez Doce, O.; Vazquez Rueda, O.; Vechernin, V.; Vercellin, E.; Vergara Limón, S.; Verma, R.; Vermunt, L.; Vértesi, R.; Verweij, M.; Vickovic, L.; Vilakazi, Z.; Villalobos Baillie, O.; Villani, A.; Vinogradov, A.; Virgili, T.; Virta, M. m. o.; Vislavicius, V.; Vodopyanov, A.; Volkel, B.; Völkl, M. a.; Voloshin, S. a.; Volpe, G.; Von Haller, B.; Vorobyev, I.; Vozniuk, N.; Vrláková, J.; Wan, J.; Wang, C.; Wang, D.; Wang, Y.; Wang, Y.; Wegrzynek, A.; Weiglhofer, F. t.; Wenzel, S. c.; Wessels, J. p.; Wiechula, J.; Wikne, J.; Wilk, G.; Wilkinson, J.; Willems, G. a.; Windelband, B.; Winn, M.; Wright, J. r.; Wu, W.; Wu, Y.; Xiong, Z.; Xu, R.; Yadav, A.; Yadav, A. k.; Yamaguchi, Y.; Yang, S.; Yano, S.; Yeats, E. r.; Yin, Z.; Yoo, I. -K.; Yoon, J. h.; Yu, H.; Yuan, S.; Yuncu, A.; Zaccolo, V.; Zampolli, C.; Zang, M.; Zandone, F.; Zardoshti, N.; Zarochentsev, A.; Závada, P.; Zaviyalov, N.; Zhalov, M.; Zhang, B.; Zhang, C.; Zhang, L.; Zhang, M.; Zhang, S.; Zhang, X.; Zhang, Y.; Zhang, Z.; Zhao, M.; Zhrebchevskii, V.; Zhi, Y.; Zhou, D.; Zhou, Y.; Zhu, J.; Zhu, S.; Zhu, Y.; Zugravel, S. c.; Zurlo, N.; Null, Null. - In: PHYSICAL REVIEW D. - ISSN 2470-0010. - STAMPA. - 110:3(2024). [10.1103/physrevd.110.032014]

Measurement of Ω_c^0 baryon production and branching-fraction ratio $\text{BR}(\Omega_c^0 \rightarrow \Omega^- e^+ \nu_e)/\text{BR}(\Omega_c^0 \rightarrow \Omega^- \pi^+)$ in pp collisions at $\sqrt{s} = 13$ TeV

S. Acharya *et al.**
(ALICE Collaboration)

 (Received 10 May 2024; accepted 24 June 2024; published 12 August 2024)

The inclusive production of the charm-strange baryon Ω_c^0 is measured for the first time via its semileptonic decay into $\Omega^- e^+ \nu_e$ at midrapidity ($|y| < 0.8$) in proton-proton (pp) collisions at the center-of-mass energy $\sqrt{s} = 13$ TeV with the ALICE detector at the LHC. The transverse momentum (p_T) differential cross section multiplied by the branching ratio is presented in the interval $2 < p_T < 12$ GeV/ c . The branching-fraction ratio $\text{BR}(\Omega_c^0 \rightarrow \Omega^- e^+ \nu_e)/\text{BR}(\Omega_c^0 \rightarrow \Omega^- \pi^+)$ is measured to be 1.12 ± 0.22 (stat) ± 0.27 (syst). Comparisons with other experimental measurements, as well as with theoretical calculations, are presented.

DOI: [10.1103/PhysRevD.110.032014](https://doi.org/10.1103/PhysRevD.110.032014)

I. INTRODUCTION

Production measurements of heavy-flavor hadrons (i.e., hadrons containing charm or beauty quarks) in high-energy proton-proton (pp) collisions provide essential tests of calculations based on the quantum chromodynamics (QCD) factorization approach [1]. These frameworks exploit the fact that the heavy-quark masses are much larger than the QCD energy scale, Λ_{QCD} , to calculate the production of heavy-flavor hadrons as a convolution of three factors: (i) the parton distribution functions (PDFs) of the incoming protons; (ii) the cross section of the partonic hard scattering; and (iii) the fragmentation functions that parametrize the nonperturbative evolution of a heavy quark into a given heavy-flavor hadron species. Heavy-quark hadronization is typically studied via the measurement of hadron-to-hadron yield ratios, because the PDFs and partonic scattering cross sections are common to the charm- or beauty- hadron species and, therefore, with appropriate choice of the scheme of calculation it can be canceled out in the yield ratios.

At the LHC, extensive production measurements of D^0 , D^+ , D_s^+ , D^{*+} charmed mesons [2–8] and of Λ_c^+ , $\Sigma_c^{0,+}$, $\Xi_c^{0,+}$, Ω_c^0 charmed baryons [9–16] have been conducted. The meson-to-meson production yield ratios, for both the respective prompt (i.e., produced in the hadronization of charm quarks or from the decay of excited open charm and charmonium states) and nonprompt (coming from beauty

hadron decays) components of the D-meson production, are observed to be independent of the transverse momentum (p_T) within uncertainties. These ratios are well described by perturbative calculations at next-to-leading order, with next-to-leading-log resummation [1,17–19], which incorporate fragmentation functions tuned on e^+e^- and e^-p collision measurements. In contrast, these calculations underestimate the observed enhancement of the production of baryons relative to mesons in hadronic collisions [20,21], with respect to the same measurements performed in e^+e^- or $e^\pm p$ collisions. Several models have been proposed to explain the baryon enhancement. They either include dynamical processes that are relevant in quark-and-gluon enriched systems (e.g., color reconnection beyond leading color approximation [22] and quark coalescence [23,24]), or that treat hadronization as a statistical process while considering a set of yet-unobserved higher-mass charm-baryon states [25].

Currently, a significant limitation in interpreting the production results of heavier strange-charm baryons is the absence of precise branching ratio measurements. In the recent inclusive $\Omega_c^0 \rightarrow \Omega^- \pi^+$ measurement reported in Ref. [16], model calculations were multiplied by the branching ratio, $\text{BR}(\Omega_c^0 \rightarrow \Omega^- \pi^+) = (0.51_{-0.31}^{+2.19})\%$. This value was obtained by considering the estimate reported in Ref. [26] for the central value, and the envelope of the values (including their uncertainties) reported in Refs. [26–30] to determine the uncertainty. This large uncertainty limited the understanding of Ω_c^0 production, meaning it is, therefore, imperative to measure its branching ratios. The Belle and CLEO Collaborations published measurements of $\text{BR}(\Omega_c^0 \rightarrow \Omega^- e^+ \nu_e)/\text{BR}(\Omega_c^0 \rightarrow \Omega^- \pi^+)$ and found 1.98 ± 0.13 (stat) ± 0.08 (syst) [31] and 2.4 ± 1.1 (stat) ± 0.2 (syst) [32], respectively. Model calculations based on the light-front approach and the light-cone sum rules predict lower values of the

*Full author list given at the end of the article.

Published by the American Physical Society under the terms of the [Creative Commons Attribution 4.0 International license](https://creativecommons.org/licenses/by/4.0/). Further distribution of this work must maintain attribution to the author(s) and the published article's title, journal citation, and DOI. Funded by SCOAP³.

branching fraction ratio of 1.1 ± 0.2 [26] and 0.71 [33], respectively. These models provide a way to relate the properties of hadrons, such as their masses, decay constants, and form factors, to fundamental QCD parameters and quark–gluon distributions within the hadrons. The hadronic part of the weak decay is parametrized in those models in terms of form factors, which belong to the nonperturbative region of QCD. Another tool to study the charmed baryon decays is based on the flavor symmetry of $SU(3)_f$ in the quark model, which allows the calculations of decay modes and relative probabilities of charmed baryon decays [34–36]. By applying the effective color approach under the framework of $SU(3)_f$ symmetry, a branching fraction ratio of 1.35 [36] is computed. The differences between the model calculations and the experimental values underscore the need for further experimental measurements and theoretical developments.

This letter presents the first p_T -differential inclusive production measurement of the semileptonic decay channel $\Omega_c^0 \rightarrow \Omega^- e^+ \nu_e$ and the branching-fraction ratio $\text{BR}(\Omega_c^0 \rightarrow \Omega^- e^+ \nu_e) / \text{BR}(\Omega_c^0 \rightarrow \Omega^- \pi^+)$ at midrapidity ($|y| < 0.8$) in pp collisions at the center-of-mass energy $\sqrt{s} = 13$ TeV. The Ω_c^0 baryon is reconstructed together with its charge conjugate in three p_T intervals, $2 < p_T < 4$ GeV/ c , $4 < p_T < 6$ GeV/ c , and $6 < p_T < 12$ GeV/ c .

II. EXPERIMENTAL SETUP AND DATA SAMPLES

The ALICE experiment and its performance are presented in detail in Refs. [37,38]. The main detectors used in this analysis are the inner tracking system (ITS) [39], the time projection chamber (TPC) [40], and the Time-Of-Flight detector (TOF) [41] for vertexing, tracking, and particle identification (PID) purposes. They are located in the central barrel covering the pseudorapidity interval ($|\eta| < 0.9$) and lie inside a solenoidal magnet that provides a magnetic field $B = 0.5$ T parallel to the beam direction. The analyzed data sample consists of pp collisions at $\sqrt{s} = 13$ TeV recorded with a minimum-bias (MB) trigger. The MB trigger requires a pair of coincident signals in two scintillator arrays (V0) [42], which are located on both sides of the nominal interaction point along the beam direction. Further offline event selection was applied to remove the contamination from beam-gas collisions and other machine-related backgrounds. These criteria were based on the timing information of the two V0 arrays and a selection on the correlation between clusters and tracklets reconstructed in the two innermost layers of the ITS (Silicon Pixel Detector, SPD). Only events with a reconstructed vertex position within ± 10 cm along the beam axis from the nominal interaction point were analyzed, to maintain a uniform ITS acceptance in pseudorapidity. The primary-vertex position was defined using tracks reconstructed in the TPC and ITS detectors. Events with

multiple reconstructed primary vertices, which amount to about 1% of the total event sample, were rejected to reduce the contamination from the superposition of several collisions within the same colliding bunches (pile-up events). After the aforementioned selection criteria, the data sample corresponds to an integrated luminosity $\mathcal{L}_{\text{int}} = (32.08 \pm 0.51) \text{ nb}^{-1}$ [43].

III. ANALYSIS METHOD

The Ω_c^0 candidates were built by pairing an electron or positron candidate track with an Ω cascade candidate using a Kalman-Filter (KF) vertexing algorithm [44]. Charge conjugate modes are included everywhere unless otherwise stated.

The Ω candidates were reconstructed via the decay chain $\Omega^- \rightarrow \Lambda K^-$ ($\text{BR} = (67.8 \pm 0.7)\%$), followed by the decay $\Lambda \rightarrow p \pi^-$ ($\text{BR} = (63.9 \pm 0.5)\%$) [45], exploiting the characteristic decay topology as reported in Refs. [16,46]. Charged-particle tracks used in this analysis were required to be within the pseudorapidity interval $|\eta| < 0.8$ and to have a number of crossed TPC pad rows larger than 70 out of a maximum of 159. Particle identification (PID) selection was based on the differences between the measured and expected response for a given particle species hypothesis, in units of the detector resolution ($n\sigma_{\text{det}}$). For proton, pion, and kaon tracks, a selection on the measured specific energy loss dE/dx in the TPC of $|n\sigma_{\text{TPC}}| < 4$ was applied for the respective particle hypothesis. An additional PID selection of $|n\sigma_{\text{TOF}}| < 5$ was applied for the kaon candidates when information from the TOF detector was available. Tracks without TOF hits were identified using only the TPC information.

Electron candidate tracks were selected by requiring to have a minimum of three (out of a maximum of six) hits in the ITS with two in the SPD layers [47,48], at least 50 clusters in the TPC, a number of crossed TPC pad rows larger than 70, and $p_T > 0.5$ GeV/ c . These requirements help suppressing the contribution from short tracks, which are unlikely to originate from the Ω_c^0 decay. The dominant source of electron background is photon conversions. They were rejected by requiring hits in the SPD layers, minimizing the effective material budget. The electron candidate tracks were identified by using dE/dx and time-of-flight information in the TPC and TOF detectors, respectively. Two selection criteria on the PID of electron candidates, $|n\sigma_{\text{TPC}}^e| < 4$ and $|n\sigma_{\text{TOF}}^e| < 5$, were required. The remaining electrons steaming from photon conversion and those originating from Dalitz decays of neutral mesons were further rejected with an invariant-mass technique [49,50]. The electron candidates were paired with opposite-sign tracks from the same event passing loose identification criteria ($|n\sigma_{\text{TPC}}^e| < 5$ without any TOF requirement) and were rejected if they formed at least one e^+e^- pairs with an invariant mass smaller than $50 \text{ MeV}/c^2$.

The Ω_c^0 candidates were selected by requiring the cosine of the opening angle between the electron and the Ω candidate tracks to be greater than 0 for $2 < p_T < 4$ GeV/c, 0.25 for $4 < p_T < 6$ GeV/c and 0.5 for $6 < p_T < 12$ GeV/c. The p_T dependence of this selection was chosen by looking at its correlation with the $e\Omega$ -pair mass distribution in data and Monte Carlo (MC) simulations, minimizing the rejection of signal candidates in the data.

After applying the selections described above, further separation of the signal and background was based on the boosted decision tree (BDT) algorithm implemented in the XGBOOST library [51,52]. Independent BDT models were trained for each p_T interval with a sample of signal and background candidates as performed in Refs [3,11,53]. For the reconstructed signal, $e\Omega$ pairs from Ω_c^0 decays were obtained from simulations with the PYTHIA 8.2 event generator [54]. Each PYTHIA event was required to contain a $c\bar{c}$ or $b\bar{b}$ quark pair and Ω_c^0 baryons were forced to decay into the $\Omega^- e^+ \nu_e$ channel. The mean proper lifetime of Ω_c^0 baryons in the simulation was set to 268 fs based on the latest LHCb measurement [55]. The transport of simulated particles within the detector was performed with the GEANT 3 package [56]. The conditions of all the ALICE detectors in terms of active channels, gain, noise level, and alignment, as well as the evolution of the detector configurations during the data-taking period, were taken into account in the simulations. A mixed-event (ME) technique was used to increase statistics in the background sample. The ME technique exploited randomized subsamples of the full dataset, using the same filtering selections described above, generating $e\Omega$ pairs with the opposite charge. The ME background was obtained by correlating Ω candidates in an event with electron candidate tracks from other events with similar multiplicity and primary-vertex position along the beam direction. Exploiting a background sample using the same-charge $e\Omega$ pairs in the same event (SE) was also

tested. The resulting background distributions were found to be consistent with each other, and the SE pairs were used to normalize the more statistically abundant ME background sample.

The BDT training variables included topological properties of the decays and PID variables. The training variables related to the PID information were obtained by combining the ones coming from the TPC and TOF, $n\sigma_{\text{combined}}^{\text{K,e}} = \frac{1}{\sqrt{2}} \sqrt{(n\sigma_{\text{TPC}}^{\text{K,e}})^2 + (n\sigma_{\text{TOF}}^{\text{K,e}})^2}$, on the electron and kaon tracks, respectively. The training variables describing the Ω decay topology were the distance of the closest approach (DCA) of the charged decay particles, the pointing angle of the reconstructed Ω momentum to the primary vertex, the $\chi_{\text{topo}}^2/\text{NDF}$, which, in this analysis, characterizes whether the momentum vector of the Ω candidate points back to the reconstructed primary vertex of the event, and the $\chi_{\text{geo}}^2/\text{NDF}$, which is related to the geometrical intersection of the daughter-particle trajectories, taking their uncertainties into account. The training variables related to the Λ were the DCA to the primary vertex, the radial distance of the Λ decay vertex from the beam axis, and the DCA between the decay particles. The BDT model output is a single response variable related to the probability that the candidate is a signal. The selection on the BDT output was tuned in each p_T interval to maximize the expected statistical significance, which was estimated using: the expected signal obtained from the Ω_c^0 production cross section reported in Ref. [16] multiplied by the BDT selection efficiency and the expected background estimated from the normalized ME. The resulting BDT output thresholds were 0.86, 0.84, and 0.81 for the three p_T intervals, respectively.

The left panel of Fig. 1 shows the invariant-mass distribution of $e\Omega$ pairs in SE (same-sign and opposite-sign) and ME (opposite-sign) in the interval $2 < p_T^{\text{e}\Omega} < 12$ GeV/c.

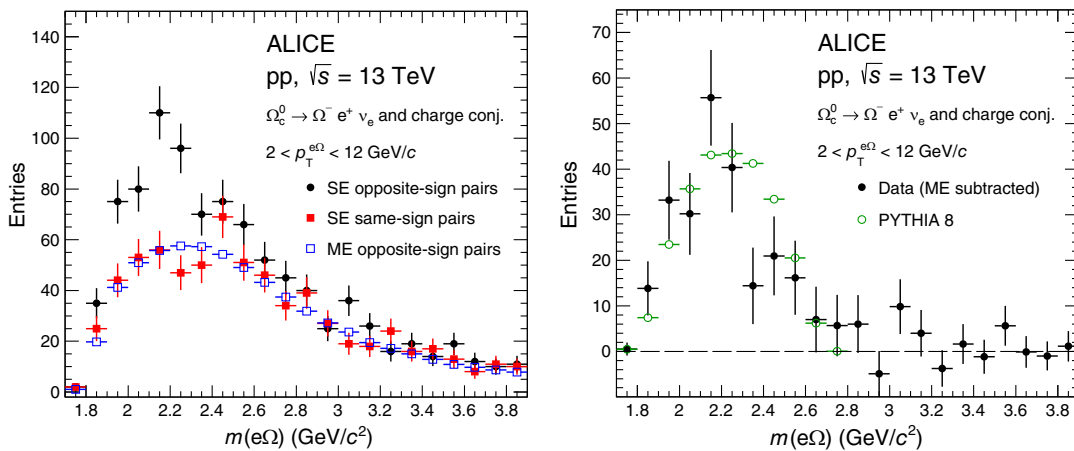


FIG. 1. Left panel: invariant-mass distribution of opposite-sign pairs (black solid circle marker) and same-sign pairs (red solid square marker) in SE, and opposite-sign pairs (blue open square marker) in ME. Right panel: invariant-mass distribution of the Ω_c^0 candidates obtained by subtracting the opposite-sign charge $e\Omega$ pairs in ME from the opposite-sign charge pairs in SE (black solid circle marker), and $e\Omega$ opposite-sign charge pairs coming from Ω_c^0 decay from PYTHIA 8 (green open circle marker).

The raw yield was obtained by subtracting the combinatorial background computed using the ME technique from the invariant-mass distribution of $e\Omega$ pairs with opposite-sign charge in the SE. The right panel of Fig. 1 shows the invariant-mass distribution of $e\Omega$ candidates, obtained after background subtraction, in comparison with $e\Omega$ opposite-sign charge pairs coming from the Ω_c^0 decay computed with the PYTHIA 8 event generator [54]. Only $e\Omega$ pairs satisfying $1.7 < m_{e\Omega} < 2.7$ GeV/ c^2 were considered for further analysis. The number of reconstructed $e\Omega$ signal pairs consists of 232 ± 15 candidates. The missing momentum of the neutrino was corrected by using the Bayesian-unfolding technique [57] implemented in the RooUnfold package [58]. The response matrix, which represents the correlation between the generated Ω_c^0 and reconstructed $e\Omega$ transverse momenta, used in the unfolding procedure is shown in the left panel of Fig. 2. In this analysis, the Bayesian procedure requires two iterations to converge. Additional information on the unfolding procedure is explained in Ref. [15]. The response matrix was determined with the same simulation setup used for the BDT training.

The p_T -differential production cross section of inclusive Ω_c^0 baryons in the rapidity interval $|y| < 0.8$ multiplied by the BR into the considered semileptonic decay channel was calculated from the yields obtained from the unfolding procedure as follows:

$$\text{BR} \times \frac{d^2 \sigma_{\Omega_c^0}}{dp_T dy} = \frac{1}{2\Delta y \Delta p_T} \times \frac{N_{\text{raw}}^{\Omega_c^0}}{(A \times \varepsilon)} \times \frac{1}{\mathcal{L}_{\text{int}}}, \quad (1)$$

where $N_{\text{raw}}^{\Omega_c^0}$ is the raw yield (sum of particles and antiparticles) in a given p_T and rapidity interval with width Δp_T and Δy . The factor 1/2 takes into account that the raw yield includes both particles and antiparticles, while the cross section is given for particles only. The \mathcal{L}_{int} is the

integrated luminosity. Since the feed-down contribution is not subtracted, the $(A \times \varepsilon)$ factor is the product of the acceptance and efficiency for inclusive Ω_c^0 baryons, where ε accounts for the reconstruction and selection of the Ω_c^0 decay-product tracks and the Ω_c^0 -candidate selection. The $(A \times \varepsilon)$ correction was obtained from a simulation with the same configuration as the one used for the BDT training and the response matrix. The $(A \times \varepsilon)$ correction factors of prompt, beauty feed-down (nonprompt), and inclusive Ω_c^0 as a function of p_T are observed to be consistent with each other within uncertainties, because the selection variables used are not sensitive to the displacement by a few hundred micrometres of the prompt and beauty feed-down Ω_c^0 decay vertices from the collision point. The Ω_c^0 -baryon p_T distribution from the PYTHIA 8 simulation was reweighted to match the true distribution, which was parametrized via a Tsallis fit to the differential production cross section of Ω_c^0 as measured in Ref. [16]. The right panel of Fig. 2 shows the product of the final $(A \times \varepsilon)$ correction factor for inclusive, prompt and feed-down Ω_c^0 as a function of p_T .

IV. SYSTEMATIC UNCERTAINTIES

The different contributions to the total systematic uncertainty of the Ω_c^0 production cross section in $2 < p_T < 12$ GeV/ c are summarized in Table I. The various systematic sources were defined as the rms of the distribution of the corrected yields obtained from the reported variations, if not differently specified.

The systematic uncertainty on the raw-yield extraction was evaluated by investigating possible contaminations to $e\Omega$ pairs with the opposite decay from other decays. The contamination of different decay channels mentioned in Refs. [32,59] are the $\Omega_c^0 \rightarrow \Xi_c^+ e^- \nu_e$, $\Xi_c^0 \rightarrow \Omega^- e^+ \nu_e K^0$, $\Xi_c^+ \rightarrow \Omega^- e^+ \nu_e K^+$, and $\Omega_c^0 \rightarrow \Omega^- e^+ \nu_e \pi^+ \pi^-$. From PYTHIA 8 simulation studies, it was found that these decays mainly

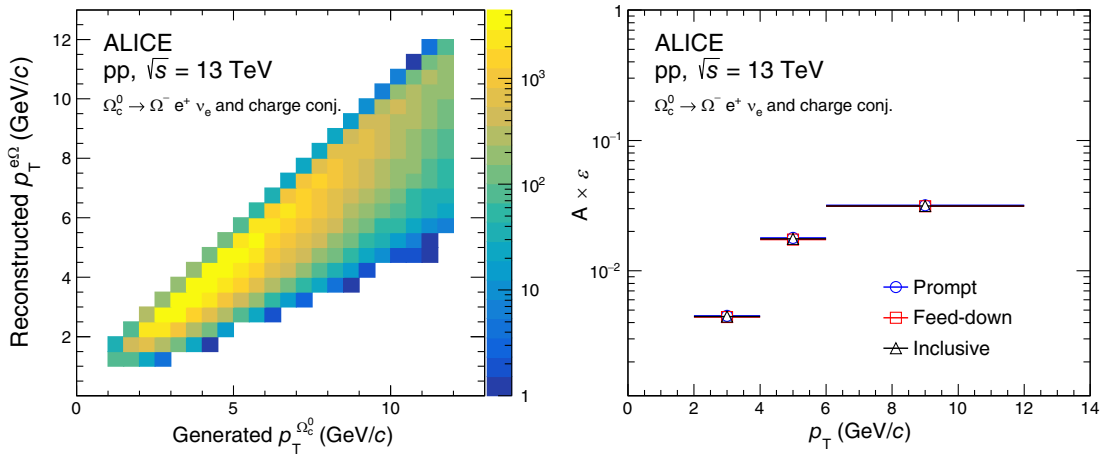


FIG. 2. Left panel: correlation matrix between the generated Ω_c^0 baryon p_T and the reconstructed opposite-sign charge pairs, obtained from the simulation based on PYTHIA 8 described in Ref. [15]. Right panel: product of $(A \times \varepsilon)$ for inclusive Ω_c^0 baryons in pp collisions at $\sqrt{s} = 13$ TeV as a function of p_T .

TABLE I. Contributions to the systematic uncertainty of the Ω_c^0 cross section for the p_T intervals $2 < p_T < 4$ GeV/ c , $4 < p_T < 6$ GeV/ c , and $6 < p_T < 12$ GeV/ c . The global uncertainty on the luminosity is quoted separately and it is not added in quadrature to the other sources.

p_T (GeV/ c)	2–4	4–6	6–12
Raw-yield extraction	10%	10%	10%
ITS–TPC matching efficiency	2%	2%	2%
Track efficiency	4%	4%	4%
Bayesian-unfolding iterations	4%	4%	4%
Unfolding method	4%	4%	4%
Response-matrix p_T range and binning	10%	10%	negl.
BDT selection	15%	15%	15%
Generated p_T shape	10%	2%	1%
Total systematic uncertainty	24%	22%	19%
Luminosity		1.6%	

contribute to a mass region below 2.2 GeV/ c^2 . A maximum variation of 10% at the corrected yield level was found by varying the lower limit of the integration mass range for the signal extraction in the $e\Omega$ mass from 1.7 to 2.2 GeV/ c^2 , which was assigned as systematic uncertainty. Note that those decay channels are not experimentally observed, therefore the Belle [31] and CLEO [32] Collaborations do not correct for it in addition to not assigning a corresponding systematic uncertainty.

The systematic uncertainty on the tracking efficiency was determined by comparing the matching efficiency of prolonging a track from the TPC to the ITS in data and simulation, and by varying the track quality selection criteria. The uncertainty on the matching efficiency, defined as the relative difference in the ITS–TPC matching efficiency between the data and simulation, affected only the electron track. For the tracks of the Ω decay particles, the prolongation to the ITS was not required. The uncertainties on electron tracks were propagated to the Ω_c^0 candidates according to the decay kinematics, resulting in an uncertainty of 2%. The second contribution to the track reconstruction was estimated by varying the track quality selection criteria and 4% uncertainty was assigned.

The systematic uncertainty on the unfolding procedure was determined by considering three contributions. The first contribution was due to the regularization procedure in the Bayesian unfolding. It was estimated by varying the iteration number between 2 and 5, and an uncertainty of 4% was assigned. The second contribution was estimated by unfolding with the singular value decomposition algorithm [60], and a 4% uncertainty was assigned, independent of Ω_c^0 p_T . The third source was related to the sensitivity of the unfolding to bin edge effects and was estimated by varying the p_T range and the binning of the response matrix. An uncertainty of 10% was assigned in the interval $2 < p_T < 6$ GeV/ c . At higher p_T , no variations were

observed when using finer p_T intervals in the unfolding procedure.

The systematic uncertainty on the selection efficiency originates from imperfections in the description of the detector response and alignment in the simulation. It was estimated from the ratios of the corrected yields obtained by varying the selections on the BDT outputs, which results in modification of the efficiencies, raw yield, and background values. The systematic evaluation was extended using a BDT model with different training variables (no PID included in the training) and preselection (PID selections were varied when not included in the BDT). A value of 15% was assigned as systematic uncertainty.

The systematic uncertainty due to the difference in the shape of the true and generated Ω_c^0 p_T distributions was estimated by varying the Tsallis fit used to determine the p_T weights within the statistical and p_T uncorrelated uncertainties. The assigned uncertainty, defined as the maximum variation observed, was 10% in the interval $2 < p_T < 4$ GeV/ c , 2% in the interval $4 < p_T < 6$ GeV/ c , and 1% for the highest p_T interval.

All systematic uncertainties are considered uncorrelated and summed in quadrature to obtain the total systematic uncertainty. The production cross section has an additional global normalization uncertainty of 1.6% due to the uncertainties of the integrated luminosity [43].

V. RESULTS

The p_T -differential cross section of inclusive Ω_c^0 baryon production multiplied by the branching ratio into $\Omega^- e^+ \nu_e$, in pp collision at $\sqrt{s} = 13$ TeV, measured in rapidity interval $|y| < 0.8$ and the p_T interval $2 < p_T < 12$ GeV/ c , is shown in the top panel of Fig. 3. It is compared with the previously published measurements of inclusive Ω_c^0 baryon production in the hadronic decay channel $\Omega_c^0 \rightarrow \Omega^- \pi^+$. The error bars and boxes represent the statistical and systematic uncertainty, respectively. The uncertainty of the integrated luminosity is not included in the boxes. In the bottom panel of Fig. 3 the branching-fraction ratio $\text{BR}(\Omega_c^0 \rightarrow \Omega^- e^+ \nu_e) / \text{BR}(\Omega_c^0 \rightarrow \Omega^- \pi^+)$ is shown as function of p_T . The systematic uncertainties on the branching-fraction ratio were calculated assuming all the uncertainties between the two measurements as uncorrelated, except for the ITS–TPC matching efficiency, track quality selection, and the MC p_T shape. The uncertainty of the luminosity cancels in the ratio, as it is fully correlated.

The ratio of the two measurements, shown in the bottom panel of Fig. 3, is used to calculate the p_T independent branching-fraction ratio. The result was averaged over p_T using the inverse uncorrelated relative uncertainties as weights [61]. The weights were defined as the sum in quadrature of the relative statistical uncertainties and the p_T -uncorrelated part of the systematic uncertainties. All the systematic uncertainties were considered as p_T -correlated

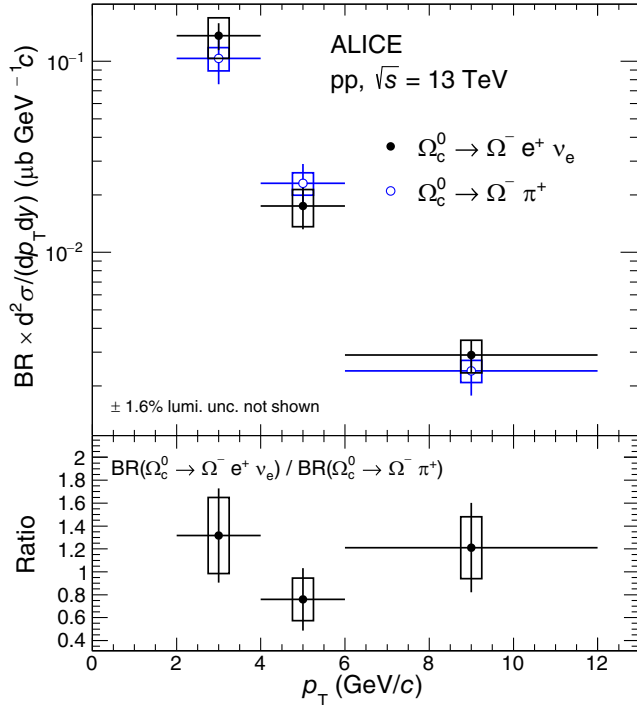


FIG. 3. Top panel: p_T -differential production cross sections of inclusive Ω_c^0 baryons multiplied by the branching ratios (BR) into $\Omega^- e^+ \nu_e$ and $\Omega^- \pi^+$ [16] in pp collisions at $\sqrt{s} = 13$ TeV. Bottom panel: p_T -differential branching-fraction ratio $BR(\Omega_c^0 \rightarrow \Omega^- e^+ \nu_e) / BR(\Omega_c^0 \rightarrow \Omega^- \pi^+)$.

in the semileptonic decay. For the hadronic decay, all systematic uncertainties were considered as p_T -correlated, except for the raw yield extraction. The p_T -correlated systematic uncertainties were propagated by recomputing the ratio after shifting up and down the ratios with the corresponding p_T -correlated systematic uncertainties. The final systematic uncertainty on the ratio is obtained by summing the p_T -correlated and uncorrelated systematic uncertainties in quadrature. The measured ratio is $BR(\Omega_c^0 \rightarrow \Omega^- e^+ \nu_e) / BR(\Omega_c^0 \rightarrow \Omega^- \pi^+) = 1.12 \pm 0.22(\text{stat}) \pm 0.27(\text{syst})$.

In Fig. 4, the measured p_T -independent branching-fraction ratio is compared with previous experimental measurements from the CLEO Collaboration [32] and Belle Collaboration [31], and with the theory predictions based on the light-front approach and light-cone sum rules calculations [26,33]. The ALICE result is compatible within 1σ with the CLEO result and is 2.3σ lower than the one measured by the Belle Collaboration. The ALICE measurement is also consistent within 1σ with the available theoretical predictions, which showed some tensions with the Belle results. The present result is also compatible within the uncertainties with the $BR(\Xi_c^0 \rightarrow \Xi^- e^+ \nu_e) / BR(\Xi_c^0 \rightarrow \Xi^- \pi^+)$ measured by the ALICE Collaboration [14]. The agreement between those two measurements is also predicted by the light-front approach calculations [26,62]. More precise measurements are expected to be performed during Runs

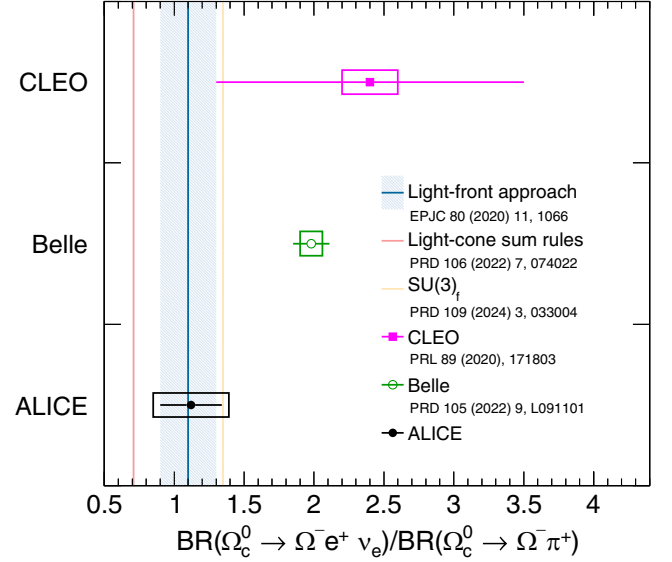


FIG. 4. Comparison of $BR(\Omega_c^0 \rightarrow \Omega^- e^+ \nu_e) / BR(\Omega_c^0 \rightarrow \Omega^- \pi^+)$ between experiments and theoretical calculations [26,31–33,36].

3 and 4 of the LHC. In view of those future measurements, it would be beneficial to compare also with additional model calculations, like LQCD [63] and RQM [64], which already provide their prediction for the branching-fraction ratio $BR(\Xi_c^0 \rightarrow \Xi^- e^+ \nu_e) / BR(\Xi_c^0 \rightarrow \Xi^- \pi^+)$.

VI. SUMMARY

The inclusive p_T -differential production cross section of the charm-baryon Ω_c^0 multiplied by the branching ratio $BR(\Omega_c^0 \rightarrow \Omega^- e^+ \nu_e)$ is measured for the first time at midrapidity ($|y| < 0.8$), in the p_T interval $2 < p_T < 12$ GeV/c , in pp collisions at $\sqrt{s} = 13$ TeV. The $BR(\Omega_c^0 \rightarrow \Omega^- e^+ \nu_e) / BR(\Omega_c^0 \rightarrow \Omega^- \pi^+)$ is measured to be $1.12 \pm 0.22(\text{stat}) \pm 0.27(\text{syst})$, using the inclusive production cross section measured in Ref. [16]. The branching-fraction ratio is consistent with theory calculations and is 2.3σ lower than the value reported by the Belle Collaboration [31].

ACKNOWLEDGMENTS

The ALICE Collaboration would like to thank all its engineers and technicians for their invaluable contributions to the construction of the experiment and the CERN accelerator teams for the outstanding performance of the LHC complex. The ALICE Collaboration gratefully acknowledges the resources and support provided by all Grid centres and the Worldwide LHC Computing Grid (WLCG) collaboration. The ALICE Collaboration acknowledges the following funding agencies for their support in building and running the ALICE detector: A. I. Alikhanyan National Science Laboratory (Yerevan Physics Institute) Foundation (ANSF), State Committee of Science

and World Federation of Scientists (WFS), Armenia; Austrian Academy of Sciences, Austrian Science Fund (FWF): [M 2467-N36] and Nationalstiftung für Forschung, Technologie und Entwicklung, Austria; Ministry of Communications and High Technologies, National Nuclear Research Center, Azerbaijan; Conselho Nacional de Desenvolvimento Científico e Tecnológico (CNPq), Financiadora de Estudos e Projetos (Finep), Fundação de Amparo à Pesquisa do Estado de São Paulo (FAPESP) and Universidade Federal do Rio Grande do Sul (UFRGS), Brazil; Bulgarian Ministry of Education and Science, within the National Roadmap for Research Infrastructures 2020-2027 (object CERN), Bulgaria; Ministry of Education of China (MOEC), Ministry of Science & Technology of China (MSTC) and National Natural Science Foundation of China (NSFC), China; Ministry of Science and Education and Croatian Science Foundation, Croatia; Centro de Aplicaciones Tecnológicas y Desarrollo Nuclear (CEADEN), Cubaenergía, Cuba; Ministry of Education, Youth and Sports of the Czech Republic, Czech Republic; The Danish Council for Independent Research | Natural Sciences, the VILLUM FONDEN and Danish National Research Foundation (DNRF), Denmark; Helsinki Institute of Physics (HIP), Finland; Commissariat à l’Energie Atomique (CEA) and Institut National de Physique Nucléaire et de Physique des Particules (IN2P3) and Centre National de la Recherche Scientifique (CNRS), France; Bundesministerium für Bildung und Forschung (BMBF) and GSI Helmholtzzentrum für Schwerionenforschung GmbH, Germany; General Secretariat for Research and Technology, Ministry of Education, Research and Religions, Greece; National Research, Development and Innovation Office, Hungary; Department of Atomic Energy Government of India (DAE), Department of Science and Technology, Government of India (DST), University Grants Commission, Government of India (UGC) and Council of Scientific and Industrial Research (CSIR), India; National Research and Innovation Agency—BRIN, Indonesia; Istituto Nazionale di Fisica Nucleare (INFN), Italy; Japanese Ministry of Education, Culture, Sports, Science and Technology (MEXT) and Japan

Society for the Promotion of Science (JSPS) KAKENHI, Japan; Consejo Nacional de Ciencia (CONACYT) y Tecnología, through Fondo de Cooperación Internacional en Ciencia y Tecnología (FONCICYT) and Dirección General de Asuntos del Personal Académico (DGAPA), Mexico; Nederlandse Organisatie voor Wetenschappelijk Onderzoek (NWO), Netherlands; The Research Council of Norway, Norway; Pontificia Universidad Católica del Perú, Peru; Ministry of Education and Science, National Science Centre and WUT ID-UB, Poland; Korea Institute of Science and Technology Information and National Research Foundation of Korea (NRF), Republic of Korea; Ministry of Education and Scientific Research, Institute of Atomic Physics, Ministry of Research and Innovation and Institute of Atomic Physics and Universitatea Nationala de Stiinta si Tehnologie Politehnica Bucuresti, Romania; Ministry of Education, Science, Research and Sport of the Slovak Republic, Slovakia; National Research Foundation of South Africa, South Africa; Swedish Research Council (VR) and Knut & Alice Wallenberg Foundation (KAW), Sweden; European Organization for Nuclear Research, Switzerland; Suranaree University of Technology (SUT), National Science and Technology Development Agency (NSTDA) and National Science, Research and Innovation Fund (NSRF via PMU-B B05F650021), Thailand; Turkish Energy, Nuclear and Mineral Research Agency (TENMAK), Turkey; National Academy of Sciences of Ukraine, Ukraine; Science and Technology Facilities Council (STFC), United Kingdom; National Science Foundation of the United States of America (NSF) and United States Department of Energy, Office of Nuclear Physics (DOE NP), United States of America. In addition, individual groups or members have received support from: Czech Science Foundation (Grant No. 23-07499S), Czech Republic; European Research Council (Grant No. 950692), European Union; ICSC—Centro Nazionale di Ricerca in High Performance Computing, Big Data and Quantum Computing, European Union—NextGenerationEU; Academy of Finland (Center of Excellence in Quark Matter) (Grants No. 346327, No. 346328), Finland.

-
- [1] M. Cacciari, M. Greco, and P. Nason, The p_T spectrum in heavy-flavor hadroproduction, *J. High Energy Phys.* **05** (1998) 007.
- [2] S. Acharya *et al.* (ALICE Collaboration), Measurement of D^0 , D^+ , D^{*+} and D_s^+ production in pp collisions at $\sqrt{s} = 5.02$ TeV with ALICE, *Eur. Phys. J. C* **79**, 388 (2019).

- [3] S. Acharya *et al.* (ALICE Collaboration), Measurement of beauty and charm production in pp collisions at $\sqrt{s} = 5.02$ TeV via non-prompt and prompt D mesons, *J. High Energy Phys.* **05** (2021) 220.
- [4] G. Aad *et al.* (ATLAS Collaboration), Measurement of $D^{*\pm}$, D^\pm and D_s^\pm meson production cross sections in

- pp collisions at $\sqrt{s} = 7$ TeV with the ATLAS detector, *Nucl. Phys.* **B907**, 717 (2016).
- [5] A. M. Sirunyan *et al.* (CMS Collaboration), Nuclear modification factor of D^0 mesons in Pb–Pb collisions at $\sqrt{s_{NN}} = 5.02$ TeV, *Phys. Lett. B* **782**, 474 (2018).
- [6] A. M. Sirunyan *et al.* (CMS Collaboration), Studies of Beauty suppression via nonprompt D^0 mesons in Pb–Pb collisions at $Q^2 = 4$ GeV², *Phys. Rev. Lett.* **123**, 022001 (2019).
- [7] R. Aaij *et al.* (LHCb Collaboration), Measurements of prompt charm production cross-sections in pp collisions at $\sqrt{s} = 5$ TeV, *J. High Energy Phys.* **06** (2017) 147.
- [8] R. Aaij *et al.* (LHCb Collaboration), Measurements of prompt charm production cross-sections in pp collisions at $\sqrt{s} = 13$ TeV, *J. High Energy Phys.* **03** (2016) 159; **09** (2016) 013(E); **05** (2017) 074(E).
- [9] S. Acharya *et al.* (ALICE Collaboration), Λ_c^+ production and baryon-to-meson ratios in pp and p–Pb collisions at $\sqrt{s_{NN}} = 5.02$ TeV at the LHC, *Phys. Rev. Lett.* **127**, 202301 (2021).
- [10] S. Acharya *et al.* (ALICE Collaboration), Λ_c^+ production in pp and in p–Pb collisions at $\sqrt{s_{NN}} = 5.02$ TeV, *Phys. Rev. C* **104**, 054905 (2021).
- [11] S. Acharya *et al.* (ALICE Collaboration), First measurement of Λ_c^+ production down to $p_T = 0$ in pp and p–Pb collisions at $\sqrt{s_{NN}} = 5.02$ TeV, *Phys. Rev. C* **107**, 064901 (2023).
- [12] A. M. Sirunyan *et al.* (CMS Collaboration), Production of Λ_c^+ baryons in proton-proton and lead–lead collisions at $\sqrt{s_{NN}} = 5.02$ TeV, *Phys. Lett. B* **803**, 135328 (2020).
- [13] S. Acharya *et al.* (ALICE Collaboration), Measurement of prompt D^0 , Λ_c^+ , and $\Sigma_c^{0,++}(2455)$ production in proton–proton collisions at $\sqrt{s} = 13$ TeV, *Phys. Rev. Lett.* **128**, 012001 (2022).
- [14] S. Acharya *et al.* (ALICE Collaboration), Measurement of the cross sections of Ξ_c^0 and Ξ_c^+ Baryons and of the branching-fraction ratio $\text{BR}(\Xi_c^0 \rightarrow \Xi^- e^+ \nu_c) / \text{BR}(\Xi_c^0 \rightarrow \Xi^- \pi^+)$ in pp collisions at $\sqrt{s} = 13$ TeV, *Phys. Rev. Lett.* **127**, 272001 (2021).
- [15] S. Acharya *et al.* (ALICE Collaboration), Measurement of the production cross section of prompt Ξ_c^0 baryons at midrapidity in pp collisions at $\sqrt{s} = 5.02$ TeV, *J. High Energy Phys.* **10** (2021) 159.
- [16] S. Acharya *et al.* (ALICE Collaboration), First measurement of Ω_c^0 production in pp collisions at $\sqrt{s} = 13$ TeV, *Phys. Lett. B* **846**, 137625 (2023).
- [17] B. A. Kniesl, G. Kramer, I. Schienbein, and H. Spiesberger, Collinear subtractions in hadroproduction of heavy quarks, *Eur. Phys. J. C* **41**, 199 (2005).
- [18] B. A. Kniesl, G. Kramer, I. Schienbein, and H. Spiesberger, Inclusive charmed-meson production at the CERN LHC, *Eur. Phys. J. C* **72**, 2082 (2012).
- [19] M. Cacciari, S. Frixione, N. Houdeau, M. L. Mangano, P. Nason, and G. Ridolfi, Theoretical predictions for charm and bottom production at the LHC, *J. High Energy Phys.* **10** (2012) 137.
- [20] S. Acharya *et al.* (ALICE Collaboration), Charm-quark fragmentation fractions and production cross section at midrapidity in pp collisions at the LHC, *Phys. Rev. D* **105**, L011103 (2022).
- [21] S. Acharya *et al.* (ALICE Collaboration), Charm production and fragmentation fractions at midrapidity in pp collisions at $\sqrt{s} = 13$ TeV, *J. High Energy Phys.* **12** (2023) 086.
- [22] J. R. Christiansen and P. Z. Skands, String formation beyond leading colour, *J. High Energy Phys.* **08** (2015) 003.
- [23] J. Song, H.-h. Li, and F.-l. Shao, New feature of low p_T charm quark hadronization in pp collisions at $\sqrt{s} = 7$ TeV, *Eur. Phys. J. C* **78**, 344 (2018).
- [24] V. Minissale, S. Plumari, and V. Greco, Charm hadrons in pp collisions at LHC energy within a coalescence plus fragmentation approach, *Phys. Lett. B* **821**, 136622 (2021).
- [25] M. He and R. Rapp, Charm-baryon production in proton-proton collisions, *Phys. Lett. B* **795**, 117 (2019).
- [26] Y.-K. Hsiao, L. Yang, C.-C. Lih, and S.-Y. Tsai, Charmed Ω_c weak decays into Ω in the light-front quark model, *Eur. Phys. J. C* **80**, 1066 (2020).
- [27] T. Gutsche, M. A. Ivanov, J. G. Körner, and V. E. Lyubovitskij, Nonleptonic two-body decays of single heavy baryons Λ_Q , Ξ_Q , and Ω_Q ($Q = b, c$) induced by W emission in the covariant confined quark model, *Phys. Rev. D* **98**, 074011 (2018).
- [28] H.-Y. Cheng, Nonleptonic weak decays of bottom baryons, *Phys. Rev. D* **56**, 2799 (1997); **99**, 079901(E) (2019).
- [29] S. Hu, G. Meng, and F. Xu, Hadronic weak decays of the charmed baryon Ω_c , *Phys. Rev. D* **101**, 094033 (2020).
- [30] K.-L. Wang, Q.-F. Lü, J.-J. Xie, and X.-H. Zhong, Toward discovering the excited Ω baryons through nonleptonic weak decays of Ω_c , *Phys. Rev. D* **107**, 034015 (2023).
- [31] Y. B. Li *et al.* (Belle Collaboration), First test of lepton flavor universality in the charmed baryon decays $\Omega_c^0 \rightarrow \Omega^- l^+ \nu_l$ using data of the Belle experiment, *Phys. Rev. D* **105**, L091101 (2022).
- [32] R. Ammar *et al.* (CLEO Collaboration), Observation of the decay $\Omega_c^0 \rightarrow \Omega^- e^+ \nu_e$, *Phys. Rev. Lett.* **89**, 171803 (2002).
- [33] T. M. Aliev, S. Bilmis, and M. Savci, Charmed baryon $\Omega_c^0 \rightarrow \Omega^- l^+ \nu_l$ and $\Omega_c^0 \rightarrow \Omega_c^- \pi^+$ (p^+) decays in light cone sum rules, *Phys. Rev. D* **106**, 074022 (2022).
- [34] C.-Q. Geng, C.-W. Liu, T.-H. Tsai, and S.-W. Yeh, Semi-leptonic decays of anti-triplet charmed baryons, *Phys. Lett. B* **792**, 214 (2019).
- [35] C. Q. Geng, Y. K. Hsiao, C.-W. Liu, and T.-H. Tsai, Three-body charmed baryon Decays with SU(3) flavor symmetry, *Phys. Rev. D* **99**, 073003 (2019).
- [36] C.-W. Liu, Nonleptonic two-body weak decays of charmed baryons, *Phys. Rev. D* **109**, 033004 (2024).
- [37] B. Abelev *et al.* (ALICE Collaboration), Performance of the ALICE experiment at the CERN LHC, *Int. J. Mod. Phys. A* **29**, 1430044 (2014).
- [38] K. Aamodt *et al.* (ALICE Collaboration), The ALICE experiment at the CERN LHC, *J. Instrum.* **3**, S08002 (2008).
- [39] K. Aamodt *et al.* (ALICE Collaboration), Alignment of the ALICE inner tracking system with cosmic-ray tracks, *J. Instrum.* **5**, P03003 (2010).
- [40] J. Alme *et al.*, The ALICE TPC, a large 3-dimensional tracking device with fast readout for ultra-high multiplicity events, *Nucl. Instrum. Methods Phys. Res., Sect. A* **622**, 316 (2010).

- [41] A. Akindinov *et al.* (ALICE Collaboration), Performance of the ALICE time-of-flight detector at the LHC, *Eur. Phys. J. Plus* **128**, 44 (2013).
- [42] E. Abbas *et al.* (ALICE Collaboration), Performance of the ALICE VZERO system, *J. Instrum.* **8**, P10016 (2013).
- [43] S. Acharya *et al.* (ALICE Collaboration), ALICE 2016-2017-2018 luminosity determination for pp collisions at $\sqrt{s} = 13$ TeV, Technical Report No. ALICE-PUBLIC-2021-005, CERN, 2021, <https://cds.cern.ch/record/2776672>.
- [44] I. Kisel, I. Kulakov, and M. Zyzak, Standalone first level event selection package for the CBM Experiment, *IEEE Trans. Nucl. Sci.* **60**, 3703 (2013).
- [45] R. L. Workman *et al.* (Particle Data Group), Review of particle physics, *Prog. Theor. Exp. Phys.* **2022**, 083C01 (2022).
- [46] S. Acharya *et al.* (ALICE Collaboration), Multiplicity dependence of (multi-)strange hadron production in proton-proton collisions at $\sqrt{s} = 13$ TeV, *Eur. Phys. J. C* **80**, 167 (2020).
- [47] S. Acharya *et al.* (ALICE Collaboration), Measurements of low- p_T electrons from semileptonic heavy-flavour hadron decays at mid-rapidity in pp and Pb-Pb collisions at $\sqrt{s_{NN}} = 2.76$ TeV, *J. High Energy Phys.* **10** (2018) 061.
- [48] S. Acharya *et al.* (ALICE Collaboration), Measurement of electrons from semileptonic heavy-flavour hadron decays at midrapidity in pp and Pb-Pb collisions at $\sqrt{s_{NN}} = 5.02$ TeV, *Phys. Lett. B* **804**, 135377 (2020).
- [49] S. Acharya *et al.* (ALICE Collaboration), Centrality and transverse momentum dependence of inclusive J/ψ production at midrapidity in Pb-Pb collisions at $\sqrt{s_{NN}} = 5.02$ TeV, *Phys. Lett. B* **805**, 135434 (2020).
- [50] S. Acharya *et al.* (ALICE Collaboration), Inclusive J/ψ production at mid-rapidity in pp collisions at $\sqrt{s} = 5.02$ TeV, *J. High Energy Phys.* **10** (2019) 084.
- [51] T. Chen and C. Guestrin, XGBoost, in *Proceedings of the 22nd ACM SIGKDD International Conference on Knowledge Discovery and Data Mining*, KDD '16 (Association for Computing Machinery, New York, NY, 2016), pp. 785–794.
- [52] L. Barioglio, F. Catalano, M. Concas, P. Fecchio, F. Grosa, F. Mazzaschi, and M. Puccio, hipe4ml/hipe4ml, [10.5281/zenodo.5734093](https://zenodo.org/record/5734093) (2021).
- [53] S. Acharya *et al.* (ALICE Collaboration), Measurement of prompt D_s^+ -meson production and azimuthal anisotropy in Pb-Pb collisions at $\sqrt{s_{NN}} = 5.02$ TeV, *Phys. Lett. B* **827**, 136986 (2022).
- [54] T. Sjöstrand, S. Ask, J. R. Christiansen, R. Corke, N. Desai, P. Ilten, S. Mrenna, S. Prestel, C. O. Rasmussen, and P. Z. Skands, An introduction to PYTHIA 8.2, *Comput. Phys. Commun.* **191**, 159 (2015).
- [55] R. Aaij *et al.* (LHCb Collaboration), Measurement of the Ω_c^0 baryon lifetime, *Phys. Rev. Lett.* **121**, 092003 (2018).
- [56] R. Brun, F. Bruyant, F. Carminati, S. Giani, M. Maire, A. McPherson, G. Patrick, and L. Urban, *GEANT: Detector Description and Simulation Tool*, CERN Program Library (CERN, Geneva, 1993).
- [57] G. D'Agostini, A Multidimensional unfolding method based on Bayes' theorem, *Nucl. Instrum. Methods Phys. Res., Sect. A* **362**, 487 (1995).
- [58] T. Auye, Unfolding algorithms and tests using RooUnfold, in *Proceedings of the PHYSTAT 2011 Workshop*, CERN-2011-006 (CERN, Geneva, Switzerland, 2011), pp. 313–318.
- [59] S. Faller and T. Mannel, Light-quark decays in heavy hadrons, *Phys. Lett. B* **750**, 653 (2015).
- [60] A. Hocker and V. Kartvelishvili, SVD approach to data unfolding, *Nucl. Instrum. Methods Phys. Res., Sect. A* **372**, 469 (1996).
- [61] M. Bonamente, *Statistics and Analysis of Scientific Data*, Graduate Texts in Physics (Springer-Verlag, New York, 2013).
- [62] Z.-X. Zhao, Weak decays of heavy baryons in the light-front approach, *Chin. Phys. C* **42**, 093101 (2018).
- [63] Q.-A. Zhang, J. Hua, F. Huang, R. Li, Y. Li, C. Lü, P. Sun, W. Sun, W. Wang, and Y. Yang, First lattice QCD calculation of semileptonic decays of charmed-strange baryons Ξ_c^* , *Chin. Phys. C* **46**, 011002 (2022).
- [64] R. N. Faustov and V. O. Galkin, Semileptonic Ξ_c baryon decays in the relativistic quark model, *Eur. Phys. J. C* **79**, 695 (2019).

S. Acharya¹²⁷, D. Adamová⁸⁶, A. Agarwal¹³⁵, G. Aglieri Rinella³², L. Aglietta^{24a,24b}, M. Agnello²⁹, N. Agrawal^{25a,25b}, Z. Ahammed¹³⁵, S. Ahmad¹⁵, S. U. Ahn⁷¹, I. Ahuja³⁷, A. Akindinov¹⁴¹, V. Akishina³⁸, M. Al-Turany⁹⁷, D. Aleksandrov¹⁴¹, B. Alessandro⁵⁶, H. M. Alfanda⁶, R. Alfaro Molina⁶⁷, B. Ali¹⁵, A. Alici^{25a,25b}, N. Alizadehvandchali¹¹⁶, A. Alkin¹⁰⁴, J. Alme²⁰, G. Alocco⁵², T. Alt⁶⁴, A. R. Altamura⁵⁰, I. Altsybeev⁹⁵, J. R. Alvarado⁴⁴, M. N. Anaam⁶, C. Andrei⁴⁵, N. Andreou¹¹⁵, A. Andronic¹²⁶, E. Andronov¹⁴¹, V. Anguelov⁹⁴, F. Antinori⁵⁴, P. Antonioli⁵¹, N. Apadula⁷⁴, L. Aphecetche¹⁰³, H. Appelshäuser⁶⁴, C. Arata⁷³, S. Arcelli^{25a,25b}, M. Aresti^{22a,22b}, R. Arnaldi⁵⁶, J. G. M. C. A. Arneiro¹¹⁰, I. C. Arsene¹⁹, M. Arslandok¹³⁸, A. Augustinus³², R. Averbeck⁹⁷, M. D. Azmi¹⁵, H. Baba¹²⁴, A. Badalà⁵³, J. Bae¹⁰⁴, Y. W. Baek⁴⁰, X. Bai¹²⁰, R. Bailhache⁶⁴, Y. Bailung⁴⁸, R. Bala⁹¹, A. Balbino²⁹, A. Baldissieri¹³⁰, B. Balis², D. Banerjee^{4a,4b}, Z. Banoo⁹¹, V. Barbasova³⁷, F. Barile^{31a,31b}, L. Barioglio⁵⁶, M. Barlou⁷⁸, B. Barman⁴¹, G. G. Barnaföldi⁴⁶, L. S. Barnby¹¹⁵, E. Barreau¹⁰³, V. Barret¹²⁷, L. Barreto¹¹⁰, C. Bartels¹¹⁹, K. Barth³², E. Bartsch⁶⁴, N. Bastid¹²⁷, S. Basu⁷⁵, G. Batigne¹⁰³, D. Battistini⁹⁵, B. Batyunya¹⁴², D. Bauri⁴⁷, J. L. Bazo Alba¹⁰¹, I. G. Bearden⁸³, C. Beattie¹³⁸, P. Becht⁹⁷, D. Behera⁴⁸, I. Belikov¹²⁹, A. D. C. Bell Hechavarria¹²⁶, F. Bellini^{25a,25b}

R. Bellwied¹¹⁶ S. Belokurova¹⁴¹ L. G. E. Beltran¹⁰⁹ Y. A. V. Beltran⁴⁴ G. Bencedi⁴⁶ A. Bensaoula¹¹⁶
S. Beole^{24a,24b} Y. Berdnikov¹⁴¹ A. Berdnikova⁹⁴ L. Bergmann⁹⁴ M. G. Besoiu⁶³ L. Betev³² P. P. Bhaduri¹³⁵
A. Bhasin⁹¹ B. Bhattacharjee⁴¹ L. Bianchi^{24a,24b} N. Bianchi⁴⁹ J. Bielčík³⁵ J. Bielčíková⁸⁶ A. P. Bigot¹²⁹
A. Bilandzic⁹⁵ G. Biro⁴⁶ S. Biswas^{4a,4b} N. Bize¹⁰³ J. T. Blair¹⁰⁸ D. Blau¹⁴¹ M. B. Blidaru⁹⁷ N. Bluhme³⁸
C. Blume⁶⁴ G. Boca^{21,55} F. Bock⁸⁷ T. Bodova²⁰ J. Bok¹⁶ L. Boldizsár⁴⁶ M. Bombara³⁷ P. M. Bond³²
G. Bonomi^{55,134} H. Borel¹³⁰ A. Borissov¹⁴¹ A. G. Borquez Carcamo⁹⁴ H. Bossi¹³⁸ E. Botta^{24a,24b}
Y. E. M. Bouziani⁶⁴ L. Bratrud⁶⁴ P. Braun-Munzinger⁹⁷ M. Bregant¹¹⁰ M. Broz³⁵ G. E. Bruno^{31a,31b,96}
M. D. Buckland^{23a,23b} D. Budnikov¹⁴¹ H. Buesching⁶⁴ S. Bufalino²⁹ P. Buhler¹⁰² N. Burmasov¹⁴¹
Z. Buthelezi^{68,123} A. Bylinkin²⁰ S. A. Bysiak¹⁰⁷ J. C. Cabanillas Noris¹⁰⁹ M. F. T. Cabrera¹¹⁶ M. Cai⁶
H. Caines¹³⁸ A. Caliva^{28a,28b} E. Calvo Villar¹⁰¹ J. M. M. Camacho¹⁰⁹ P. Camerini^{23a,23b} F. D. M. Canedo¹¹⁰
S. L. Cantway¹³⁸ M. Carabas¹¹³ A. A. Carballo³² F. Carnesecchi³² R. Caron¹²⁸ L. A. D. Carvalho¹¹⁰
J. Castillo Castellanos¹³⁰ M. Castoldi³² F. Catalano³² S. Cattaruzzi^{23a,23b} C. Ceballos Sanchez¹⁴² R. Cerri^{24a,24b}
I. Chakaberia⁷⁴ P. Chakraborty^{47,136} S. Chandra¹³⁵ S. Chapeland³² M. Chartier¹¹⁹ S. Chattopadhyay¹³⁵
S. Chattopadhyay¹³⁵ S. Chattopadhyay⁹⁹ T. Cheng^{6,97} C. Cheshkov¹²⁸ V. Chibante Barroso³²
D. D. Chinellato¹¹¹ E. S. Chizzali^{95,‡} J. Cho⁵⁸ S. Cho⁵⁸ P. Chochula³² Z. A. Chochulska¹³⁶ D. Choudhury⁴¹
P. Christakoglou⁸⁴ C. H. Christensen⁸³ P. Christiansen⁷⁵ T. Chujo¹²⁵ M. Ciacco²⁹ C. Cicalo⁵² M. R. Ciupek⁹⁷
G. Clai^{51,§} F. Colamaria⁵⁰ J. S. Colburn¹⁰⁰ D. Colella^{31a,31b} M. Colocci^{25a,25b} M. Concas³²
G. Conesa Balbastre⁷³ Z. Conesa del Valle¹³¹ G. Contin^{23a,23b} J. G. Contreras³⁵ M. L. Coquet^{103,130}
P. Cortese^{56,133} M. R. Cosentino¹¹² F. Costa³² S. Costanza^{21,55} C. Cot¹³¹ J. Crkovská⁹⁴ P. Crochet¹²⁷
R. Cruz-Torres⁷⁴ P. Cui⁶ M. M. Czarnynoga¹³⁶ A. Dainese⁵⁴ G. Dange³⁸ M. C. Danisch⁹⁴ A. Danu⁶³ P. Das⁸⁰
P. Das^{4a,4b} S. Das^{4a,4b} A. R. Dash¹²⁶ S. Dash⁴⁷ A. De Caro^{28a,28b} G. de Cataldo⁵⁰ J. de Cuveland³⁸
A. De Falco^{22a,22b} D. De Gruttola^{28a,28b} N. De Marco⁵⁶ C. De Martin^{23a,23b} S. De Pasquale^{28a,28b} R. Deb¹³⁴
R. Del Grande⁹⁵ L. Dello Stritto³² W. Deng⁶ K. C. Devereaux¹⁸ P. Dhankher¹⁸ D. Di Bari^{31a,31b}
A. Di Mauro³² B. Diab¹³⁰ R. A. Diaz^{7,142} T. Dietel¹¹⁴ Y. Ding⁶ J. Ditzel⁶⁴ R. Divià³² Ø. Djuvsland²⁰
U. Dmitrieva¹⁴¹ A. Dobrin⁶³ B. Dönigus⁶⁴ J. M. Dubinski¹³⁶ A. Dubla⁹⁷ P. Dupieux¹²⁷ N. Dzalaiova¹³
T. M. Eder¹²⁶ R. J. Ehlers⁷⁴ F. Eisenhut⁶⁴ R. Ejima⁹² D. Elia⁵⁰ B. Erazmus¹⁰³ F. Ercolessi^{25a,25b}
B. Espagnon¹³¹ G. Eulisse³² D. Evans¹⁰⁰ S. Evdokimov¹⁴¹ L. Fabbietti⁹⁵ M. Faggin^{27a,27b} J. Faivre⁷³
F. Fan⁶ W. Fan⁷⁴ A. Fantoni⁴⁹ M. Fasel⁸⁷ A. Feliciello⁵⁶ G. Feofilov¹⁴¹ A. Fernández Téllez⁴⁴
L. Ferrandi¹¹⁰ M. B. Ferrer³² A. Ferrero¹³⁰ C. Ferrero^{56,||} A. Ferretti^{24a,24b} V. J. G. Feuillard⁹⁴ V. Filova³⁵
D. Finogeev¹⁴¹ F. M. Fionda⁵² E. Flatland³² F. Flor¹¹⁶ A. N. Flores¹⁰⁸ S. Foertsch⁶⁸ I. Fokin⁹⁴ S. Fokin¹⁴¹
U. Follo^{56,||} E. Fragiaco⁵⁷ E. Frajna⁴⁶ U. Fuchs³² N. Funicello^{28a,28b} C. Furget⁷³ A. Furs¹⁴¹
T. Fusayasu⁹⁸ J. J. Gaardhøje⁸³ M. Gagliardi^{24a,24b} A. M. Gago¹⁰¹ T. Gahlaut⁴⁷ C. D. Galvan¹⁰⁹
D. R. Gangadharan¹¹⁶ P. Ganoti⁷⁸ C. Garabatos⁹⁷ J. M. Garcia⁴⁴ T. García Chávez⁴⁴ E. Garcia-Solis⁹
C. Gargiulo³² P. Gasik⁹⁷ H. M. Gaur³⁸ A. Gautam¹¹⁸ M. B. Gay Ducati⁶⁶ M. Germain¹⁰³ C. Ghosh¹³⁵
M. Giacalone⁵¹ G. Gioachin²⁹ P. Giubellino^{56,97} P. Giubilato^{27a,27b} A. M. C. Glaenger¹³⁰ P. Glässel⁹⁴
E. Glimos¹²² D. J. Q. Goh⁷⁶ V. Gonzalez¹³⁷ P. Gordeev¹⁴¹ M. Gorgon² K. Goswami⁴⁸ S. Gotovac³³
V. Grabski⁶⁷ L. K. Graczykowski¹³⁶ E. Grecka⁸⁶ A. Grelli⁵⁹ C. Grigoras³² V. Grigoriev¹⁴¹ S. Grigoryan^{1,142}
F. Grosa³² J. F. Grosse-Oetringhaus³² R. Grosso⁹⁷ D. Grund³⁵ N. A. Grunwald⁹⁴ G. G. Guardiano¹¹¹
R. Guernane⁷³ M. Guilbaud¹⁰³ K. Gulbrandsen⁸³ J. J. W. K. Gumprecht¹⁰² T. Gündem⁶⁴ T. Gunji¹²⁴ W. Guo⁶
A. Gupta⁹¹ R. Gupta⁹¹ R. Gupta⁴⁸ K. Gwizdziel¹³⁶ L. Gyulai⁴⁶ C. Hadjidakis¹³¹ F. U. Haider⁹¹
S. Haidlova³⁵ M. Haldar^{4a,4b} H. Hamagaki⁷⁶ A. Hamdi⁷⁴ Y. Han¹³⁹ B. G. Hanley¹³⁷ R. Hannigan¹⁰⁸
J. Hansen⁷⁵ M. R. Haque⁹⁷ J. W. Harris¹³⁸ A. Harton⁹ M. V. Hartung⁶⁴ H. Hassan¹¹⁷ D. Hatzifotiadou⁵¹
P. Hauer⁴² L. B. Havener¹³⁸ E. Hellbär⁹⁷ H. Helstrup³⁴ M. Hemmer⁶⁴ T. Herman³⁵ S. G. Hernandez¹¹⁶
G. Herrera Corral⁸ S. Herrmann¹²⁸ K. F. Hetland³⁴ B. Heybeck⁶⁴ H. Hillemanns³² B. Hippolyte¹²⁹
F. W. Hoffmann⁷⁰ B. Hofman⁵⁹ G. H. Hong¹³⁹ M. Horst⁹⁵ A. Horzyk² Y. Hou⁶ P. Hristov³² P. Huhn⁶⁴
L. M. Huhta¹¹⁷ T. J. Humanic⁸⁸ A. Hutson¹¹⁶ D. Hutter³⁸ M. C. Hwang¹⁸ R. Ilkaev¹⁴¹ M. Inaba¹²⁵
G. M. Innocenti³² M. Ippolitov¹⁴¹ A. Isakov⁸⁴ T. Isidori¹¹⁸ M. S. Islam⁹⁹ S. Iurchenko¹⁴¹ M. Ivanov⁹⁷
M. Ivanov¹³ V. Ivanov¹⁴¹ K. E. Iversen⁷⁵ M. Jablonski² B. Jacak^{18,74} N. Jacazio^{25a,25b} P. M. Jacobs⁷⁴
S. Jadlovská¹⁰⁶ J. Jadlovsky¹⁰⁶ S. Jaelani⁸² C. Jahnke¹¹⁰ M. J. Jakubowska¹³⁶ M. A. Janik¹³⁶ T. Janson⁷⁰ S. Ji¹⁶

S. Jia¹⁰, A. A. P. Jimenez⁶⁵, F. Jonas⁷⁴, D. M. Jones¹¹⁹, J. M. Jowett^{32,97}, J. Jung⁶⁴, M. Jung⁶⁴, A. Junique³², A. Jusko¹⁰⁰, J. Kaewjai¹⁰⁵, P. Kalinak⁶⁰, A. Kalweit³², A. Karasu Uysal^{72,¶}, D. Karatovic⁸⁹, N. Karatzenis¹⁰⁰, O. Karavichev¹⁴¹, T. Karavicheva¹⁴¹, E. Karpechev¹⁴¹, M. J. Karwowska^{32,136}, U. Keschull⁷⁰, R. Keidel¹⁴⁰, M. Keil³², B. Ketzer⁴², S. S. Khade⁴⁸, A. M. Khan¹²⁰, S. Khan¹⁵, A. Khazadeev¹⁴¹, Y. Kharlov¹⁴¹, A. Khatun¹¹⁸, A. Khuntia³⁵, Z. Khuranova⁶⁴, B. Kileng³⁴, B. Kim¹⁰⁴, C. Kim¹⁶, D. J. Kim¹¹⁷, E. J. Kim⁶⁹, J. Kim¹³⁹, J. Kim⁵⁸, J. Kim^{32,69}, M. Kim¹⁸, S. Kim¹⁷, T. Kim¹³⁹, K. Kimura⁹², A. Kirkova³⁶, S. Kirsch⁶⁴, I. Kisel³⁸, S. Kiselev¹⁴¹, A. Kisiel¹³⁶, J. P. Kitowski², J. L. Klay⁵, J. Klein³², S. Klein⁷⁴, C. Klein-Bösing¹²⁶, M. Kleiner⁶⁴, T. Klemenz⁹⁵, A. Kluge³², C. Kobdaj¹⁰⁵, R. Kohara¹²⁴, T. Kollegger⁹⁷, A. Kondratyev¹⁴², N. Kondratyeva¹⁴¹, J. König⁶⁴, S. A. Königstorfer⁹⁵, P. J. Konopka³², G. Kornakov¹³⁶, M. Korwieser⁹⁵, S. D. Koryciak², C. Koster⁸⁴, A. Kotliarov⁸⁶, N. Kovacic⁸⁹, V. Kovalenko¹⁴¹, M. Kowalski¹⁰⁷, V. Kozhuharov³⁶, I. Králík⁶⁰, A. Kravčáková³⁷, L. Krcal^{32,38}, M. Krivda^{60,100}, F. Krizek⁸⁶, K. Krizkova Gajdosova³², C. Krug⁶⁶, M. Krüger⁶⁴, D. M. Krupova³⁵, E. Kryshen¹⁴¹, V. Kučera⁵⁸, C. Kuhn¹²⁹, P. G. Kuijper⁸⁴, T. Kumaoka¹²⁵, D. Kumar¹³⁵, L. Kumar⁹⁰, N. Kumar⁹⁰, S. Kumar^{31a,31b}, S. Kundu³², P. Kurashvili⁷⁹, A. Kurepin¹⁴¹, A. B. Kurepin¹⁴¹, A. Kuryakin¹⁴¹, S. Kushpil⁸⁶, V. Kuskov¹⁴¹, M. Kutyla¹³⁶, M. J. Kweon⁵⁸, Y. Kwon¹³⁹, S. L. La Pointe³⁸, P. La Rocca^{26a,26b}, A. Lakrathok¹⁰⁵, M. Lamanna³², A. R. Landou⁷³, R. Langoy¹²¹, P. Larionov³², E. Laudi³², L. Lautner^{32,95}, R. A. N. Laveaga¹⁰⁹, R. Lavicka¹⁰², R. Lea^{55,134}, H. Lee¹⁰⁴, I. Legrand⁴⁵, G. Legras¹²⁶, J. Lehrbach³⁸, T. M. Lelek², R. C. Lemmon⁸⁵, I. León Monzón¹⁰⁹, M. M. Lesch⁹⁵, E. D. Lesser¹⁸, P. Lévai⁴⁶, M. Li⁶, X. Li¹⁰, B. E. Liang-gilman¹⁸, J. Lien¹²¹, R. Lietava¹⁰⁰, I. Likmeta¹¹⁶, B. Lim^{24a,24b}, S. H. Lim¹⁶, V. Lindenstruth³⁸, A. Lindner⁴⁵, C. Lippmann⁹⁷, D. H. Liu⁶, J. Liu¹¹⁹, G. S. S. Liveraro¹¹¹, I. M. Lofnes²⁰, C. Loizides⁸⁷, S. Lokos¹⁰⁷, J. Lömker⁵⁹, X. Lopez¹²⁷, E. López Torres⁷, P. Lu^{97,120}, F. V. Lugo⁶⁷, J. R. Luhder¹²⁶, M. Lunardon^{27a,27b}, G. Luparello⁵⁷, Y. G. Ma³⁹, M. Mager³², A. Maire¹²⁹, E. M. Majerz², M. V. Makariev³⁶, M. Malaev¹⁴¹, G. Malfattore^{25a,25b}, N. M. Malik⁹¹, Q. W. Malik¹⁹, S. K. Malik⁹¹, L. Malinina^{142,†}, D. Mallick¹³¹, N. Mallick⁴⁸, G. Mandaglio^{30,53}, S. K. Mandal⁷⁹, A. Manea⁶³, V. Manko¹⁴¹, F. Manso¹²⁷, V. Manzari⁵⁰, Y. Mao⁶, R. W. Marcjan², G. V. Margagliotti^{23a,23b}, A. Margotti⁵¹, A. Marín⁹⁷, C. Markert¹⁰⁸, P. Martinengo³², M. I. Martínez⁴⁴, G. Martínez García¹⁰³, M. P. P. Martins¹¹⁰, S. Masciocchi⁹⁷, M. Masera^{24a,24b}, A. Masoni⁵², L. Massacrier¹³¹, O. Massen⁵⁹, A. Mastroserio^{50,132}, O. Matonoha⁷⁵, S. Mattiazzo^{27a,27b}, A. Matyja¹⁰⁷, A. L. Mazuecos³², F. Mazzaschi^{24a,24b,32}, M. Mazzilli¹¹⁶, J. E. Mdhluli¹²³, Y. Melikyan⁴³, A. Menchaca-Rocha⁶⁷, J. E. M. Mendez⁶⁵, E. Meninno¹⁰², A. S. Menon¹¹⁶, M. W. Menzel^{32,94}, M. Meres¹³, Y. Miake¹²⁵, L. Micheletti³², D. L. Mihaylov⁹⁵, K. Mikhaylov^{141,142}, N. Minafra¹¹⁸, D. Miśkowiec⁹⁷, A. Modak^{4a,4b,134}, B. Mohanty⁸⁰, M. Mohisin Khan^{15,**}, M. A. Molander⁴³, S. Monira¹³⁶, C. Mordasini¹¹⁷, D. A. Moreira De Godoy¹²⁶, I. Morozov¹⁴¹, A. Morsch³², T. Mrnjavac³², V. Muccifora⁴⁹, S. Muhuri¹³⁵, J. D. Mulligan⁷⁴, A. Mulliri^{22a,22b}, M. G. Munhoz¹¹⁰, R. H. Munzer⁶⁴, H. Murakami¹²⁴, S. Murray¹¹⁴, L. Musa³², J. Musinsky⁶⁰, J. W. Myrcha¹³⁶, B. Naik¹²³, A. I. Nambrath¹⁸, B. K. Nandi⁴⁷, R. Nania⁵¹, E. Nappi⁵⁰, A. F. Nassirpour¹⁷, A. Nath⁹⁴, C. Nattress¹²², M. N. Naydenov³⁶, A. Neagu¹⁹, A. Negru¹¹³, E. Nekrasova¹⁴¹, L. Nellen⁶⁵, R. Nepeivoda⁷⁵, S. Nese¹⁹, G. Neskovic³⁸, N. Nicassio⁵⁰, B. S. Nielsen⁸³, E. G. Nielsen⁸³, S. Nikolaev¹⁴¹, S. Nikulin¹⁴¹, V. Nikulin¹⁴¹, F. Noferini⁵¹, S. Noh¹², P. Nomokonov¹⁴², J. Norman¹¹⁹, N. Novitzky⁸⁷, P. Nowakowski¹³⁶, A. Nyanin¹⁴¹, J. Nystrand²⁰, S. Oh¹⁷, A. Ohlson⁷⁵, V. A. Okorokov¹⁴¹, J. Oleniacz¹³⁶, A. Onnerstad¹¹⁷, C. Oppedisano⁵⁶, A. Ortiz Velasquez⁶⁵, J. Otwinowski¹⁰⁷, M. Oya⁹², K. Oyama⁷⁶, Y. Pachmayer⁹⁴, S. Padhan⁴⁷, D. Pagano^{55,134}, G. Paic⁶⁵, S. Paisano-Guzmán⁴⁴, A. Palasciano⁵⁰, S. Panebianco¹³⁰, H. Park¹²⁵, H. Park¹⁰⁴, J. Park¹²⁵, J. E. Parkkila³², Y. Patley⁴⁷, B. Paul^{22a,22b}, M. M. D. M. Paulino¹¹⁰, H. Pei⁶, T. Peitzmann⁵⁹, X. Peng¹¹, M. Pennisi^{24a,24b}, S. Perciballi^{24a,24b}, D. Peresunko¹⁴¹, G. M. Perez⁷, Y. Pestov¹⁴¹, M. T. Petersen⁸³, V. Petrov¹⁴¹, M. Petrovici⁴⁵, S. Piano⁵⁷, M. Pikna¹³, P. Pillot¹⁰³, O. Pinazza^{32,51}, L. Pinsky¹¹⁶, C. Pinto⁹⁵, S. Pisano⁴⁹, M. Płoskoń⁷⁴, M. Planinic⁸⁹, F. Pliquett⁶⁴, M. G. Poghosyan⁸⁷, B. Polichtchouk¹⁴¹, S. Politano²⁹, N. Poljak⁸⁹, A. Pop⁴⁵, S. Porteboeuf-Houssais¹²⁷, V. Pozdniakov^{142,†}, I. Y. Pozos⁴⁴, K. K. Pradhan⁴⁸, S. K. Prasad^{4a,4b}, S. Prasad⁴⁸, R. Preghenella⁵¹, F. Prino⁵⁶, C. A. Pruneau¹³⁷, I. Pshenichnov¹⁴¹, M. Puccio³², S. Pucillo^{24a,24b}, S. Qiu⁸⁴, L. Quaglia^{24a,24b}, S. Ragoni¹⁴, A. Rai¹³⁸, A. Rakotozafindrabe¹³⁰, L. Ramello^{56,133}, F. Rami¹²⁹, M. Rasa^{26a,26b}, S. S. Räsänen⁴³, R. Rath⁵¹, M. P. Rauch²⁰, I. Ravasenga³², K. F. Read^{87,122}, C. Reckziegel¹¹², A. R. Redelbach³⁸, K. Redlich^{79,†}, C. A. Reetz⁹⁷, H. D. Regules-Medel⁴⁴, A. Rehman²⁰, F. Reidt³²

H. A. Reme-Ness³⁴, Z. Rescakova,³⁷ K. Reygers⁹⁴, A. Riabov¹⁴¹, V. Riabov¹⁴¹, R. Ricci^{28a,28b}, M. Richter²⁰,
A. A. Riedel⁹⁵, W. Riegler³², A. G. Riffero^{24a,24b}, C. Ripoli,^{28a,28b} C. Ristea⁶³, M. V. Rodriguez³²,
M. Rodríguez Cahuantzi⁴⁴, S. A. Rodríguez Ramírez⁴⁴, K. Røed¹⁹, R. Rogalev¹⁴¹, E. Rogochaya¹⁴²,
T. S. Rogoschinski⁶⁴, D. Rohr³², D. Röhrich²⁰, S. Rojas Torres³⁵, P. S. Rokita¹³⁶, G. Romanenko^{25a,25b},
F. Ronchetti⁴⁹, E. D. Rosas,⁶⁵ K. Roslon¹³⁶, A. Rossi⁵⁴, A. Roy⁴⁸, S. Roy⁴⁷, N. Rubini^{25a,25b}, J. A. Rudolph,⁸⁴
D. Ruggiano¹³⁶, R. Rui^{23a,23b}, P. G. Russek², R. Russo⁸⁴, A. Rustamov⁸¹, E. Ryabinkin¹⁴¹, Y. Ryabov¹⁴¹,
A. Rybicki¹⁰⁷, J. Ryu¹⁶, W. Rzesza¹³⁶, S. Sadhu^{31a,31b}, S. Sadovsky¹⁴¹, J. Saetre²⁰, K. Šafařík³⁵, S. K. Saha^{4a,4b},
S. Saha⁸⁰, B. Sahoo⁴⁸, R. Sahoo⁴⁸, S. Sahoo⁶¹, D. Sahu⁴⁸, P. K. Sahu⁶¹, J. Saini¹³⁵, K. Sajdakova,³⁷ S. Sakai¹²⁵,
M. P. Salvan⁹⁷, S. Sambyal⁹¹, D. Samitz¹⁰², I. Sanna^{32,95}, T. B. Saramela,¹¹⁰ D. Sarkar⁸³, P. Sarma⁴¹,
V. Sarritzu^{22a,22b}, V. M. Sarti⁹⁵, M. H. P. Sas³², S. Sawan⁸⁰, E. Scapparone⁵¹, J. Schambach⁸⁷, H. S. Scheid⁶⁴,
C. Schiaua⁴⁵, R. Schicker⁹⁴, F. Schlepfer⁹⁴, A. Schmah,⁹⁷ C. Schmidt⁹⁷, H. R. Schmidt,⁹³ M. O. Schmidt³²,
M. Schmidt,⁹³ N. V. Schmidt⁸⁷, A. R. Schmier¹²², R. Schotter¹²⁹, A. Schröter³⁸, J. Schukraft³², K. Schweda⁹⁷,
G. Scioli^{25a,25b}, E. Scomparin⁵⁶, J. E. Seger¹⁴, Y. Sekiguchi,¹²⁴ D. Sekihata¹²⁴, M. Selina⁸⁴, I. Selyuzhenkov⁹⁷,
S. Senyukov¹²⁹, J. J. Seo⁹⁴, D. Serebryakov¹⁴¹, L. Serkin⁶⁵, L. Šerkšnytė⁹⁵, A. Sevcenco⁶³, T. J. Shaba⁶⁸,
A. Shabetai¹⁰³, R. Shahoyan,³² A. Shangaraev¹⁴¹, B. Sharma⁹¹, D. Sharma⁴⁷, H. Sharma⁵⁴, M. Sharma⁹¹,
S. Sharma⁷⁶, S. Sharma⁹¹, U. Sharma⁹¹, A. Shatat¹³¹, O. Sheibani,¹¹⁶ K. Shigaki⁹², M. Shimomura,⁷⁷ J. Shin,¹²
S. Shirinkin¹⁴¹, Q. Shou³⁹, Y. Sibiriak¹⁴¹, S. Siddhanta⁵², T. Siemiarzczuk⁷⁹, T. F. Silva¹¹⁰, D. Silvermyr⁷⁵,
T. Simantathammakul,¹⁰⁵ R. Simeonov³⁶, B. Singh,⁹¹ B. Singh⁹⁵, K. Singh⁴⁸, R. Singh⁸⁰, R. Singh⁹¹,
R. Singh^{48,97}, S. Singh¹⁵, V. K. Singh¹³⁵, V. Singhal¹³⁵, T. Sinha⁹⁹, B. Sitar¹³, M. Sitta^{56,133}, T. B. Skaali,¹⁹
G. Skorodumovs⁹⁴, N. Smirnov¹³⁸, R. J. M. Snellings⁵⁹, E. H. Solheim¹⁹, J. Song¹⁶, C. Sonnabend^{32,97},
J. M. Sonneveld⁸⁴, F. Soramel^{27a,27b}, A. B. Soto-hernandez⁸⁸, R. Spijkers⁸⁴, I. Sputowska¹⁰⁷, J. Staa⁷⁵,
J. Stachel⁹⁴, I. Stan⁶³, P. J. Steffanic¹²², S. F. Stiefelmaier⁹⁴, D. Stocco¹⁰³, I. Storehaug¹⁹, N. J. Strangmann⁶⁴,
P. Stratmann¹²⁶, S. Strazzi^{25a,25b}, A. Sturniolo^{30,53}, C. P. Stylianidis,⁸⁴ A. A. P. Suaide¹¹⁰, C. Suire¹³¹,
M. Sukhanov¹⁴¹, M. Suljic³², R. Sultanov¹⁴¹, V. Sumberia⁹¹, S. Sumowidagdo⁸², I. Szarka¹³,
M. Szymkowski¹³⁶, S. F. Taghavi⁹⁵, G. TAILLEPIED⁹⁷, J. Takahashi¹¹¹, G. J. Tambave⁸⁰, S. Tang⁶, Z. Tang¹²⁰,
J. D. Tapia Takaki¹¹⁸, N. Tapus,¹¹³ L. A. Tarasovicova¹²⁶, M. G. Tarzila⁴⁵, G. F. Tassielli^{31a,31b}, A. Tauro³²,
A. Tavira García¹³¹, G. Tejada Muñoz⁴⁴, A. Telesca³², L. Terlizzi^{24a,24b}, C. Terrevoli⁵⁰, S. Thakur^{4a,4b},
D. Thomas¹⁰⁸, A. Tikhonov¹⁴¹, N. Tiltmann^{32,126}, A. R. Timmins¹¹⁶, M. Tkacik¹⁰⁶, T. Tkacik¹⁰⁶, A. Toia⁶⁴,
R. Tokumoto,⁹² S. Tomassini,^{25a,25b} K. Tomohiro,⁹² N. Topilskaya¹⁴¹, M. Toppi⁴⁹, T. Tork¹³¹, V. V. Torres¹⁰³,
A. G. Torres Ramos^{31a,31b}, A. Trifiró^{30,53}, T. Triloki,⁹⁶ A. S. Triolo^{30,32,53}, S. Tripathy³², T. Tripathy⁴⁷,
V. Trubnikov³, W. H. Trzaska¹¹⁷, T. P. Trzcinski¹³⁶, C. Tsolanta,¹⁹ A. Tumkin¹⁴¹, R. Turrisi⁵⁴, T. S. Tveter¹⁹,
K. Ullaland²⁰, B. Ulukutlu⁹⁵, A. Uras¹²⁸, M. Urioni¹³⁴, G. L. Usai^{22a,22b}, M. Vala,³⁷ N. Valle⁵⁵,
L. V. R. van Doremalen,⁵⁹ M. van Leeuwen⁸⁴, C. A. van Veen⁹⁴, R. J. G. van Weelden⁸⁴, P. Vande Vyvre³²,
D. Varga⁴⁶, Z. Varga⁴⁶, P. Vargas Torres,⁶⁵ M. Vasileiou⁷⁸, A. Vasiliev¹⁴¹, O. Vázquez Doce⁴⁹,
O. Vazquez Rueda¹¹⁶, V. Vechernin¹⁴¹, E. Vercellin^{24a,24b}, S. Vergara Limón,⁴⁴ R. Verma,⁴⁷ L. Vermunt⁹⁷,
R. Vértési⁴⁶, M. Verweij⁵⁹, L. Vickovic,³³ Z. Vilakazi,¹²³ O. Villalobos Baillie¹⁰⁰, A. Villani^{23a,23b},
A. Vinogradov¹⁴¹, T. Virgili^{28a,28b}, M. M. O. Virta¹¹⁷, V. Vislavicius,⁷⁵ A. Vodopyanov¹⁴², B. Volkel³²,
M. A. Völkl⁹⁴, S. A. Voloshin¹³⁷, G. Volpe^{31a,31b}, B. von Haller³², I. Vorobyev³², N. Vozniuk¹⁴¹, J. Vrláková³⁷,
J. Wan,³⁹ C. Wang³⁹, D. Wang,³⁹ Y. Wang³⁹, Y. Wang⁶, A. Wegrzynek³², F. T. Weiglhofer,³⁸ S. C. Wenzel³²,
J. P. Wessels¹²⁶, J. Wiechula⁶⁴, J. Wikne¹⁹, G. Wilk⁷⁹, J. Wilkinson⁹⁷, G. A. Willems¹²⁶, B. Windelband⁹⁴,
M. Winn¹³⁰, J. R. Wright¹⁰⁸, W. Wu,³⁹ Y. Wu¹²⁰, Z. Xiong,¹²⁰ R. Xu⁶, A. Yadav⁴², A. K. Yadav¹³⁵,
Y. Yamaguchi⁹², S. Yang,²⁰ S. Yano⁹², E. R. Yeats,¹⁸ Z. Yin⁶, I.-K. Yoo¹⁶, J. H. Yoon⁵⁸, H. Yu,¹² S. Yuan,²⁰
A. Yuncu⁹⁴, V. Zaccolo^{23a,23b}, C. Zampolli³², M. Zang,⁶ F. Zanone⁹⁴, N. Zardoshti³², A. Zarochentsev¹⁴¹,
P. Závada⁶², N. Zaviyalov,¹⁴¹ M. Zhalov¹⁴¹, B. Zhang⁶, C. Zhang¹³⁰, L. Zhang³⁹, M. Zhang,^{6,127} S. Zhang³⁹,
X. Zhang⁶, Y. Zhang,¹²⁰ Z. Zhang⁶, M. Zhao¹⁰, V. Zherebchevskii¹⁴¹, Y. Zhi,¹⁰ D. Zhou⁶, Y. Zhou⁸³, J. Zhu^{6,54},
S. Zhu,¹²⁰ Y. Zhu,⁶ S. C. Zugravel⁵⁶ and N. Zurlo^{55,134}

(ALICE Collaboration)

- ¹A.I. Alikhanyan National Science Laboratory (Yerevan Physics Institute) Foundation, Yerevan, Armenia
²AGH University of Krakow, Cracow, Poland
³Bogolyubov Institute for Theoretical Physics, National Academy of Sciences of Ukraine, Kiev, Ukraine
^{4a}Bose Institute, Department of Physics, Kolkata, India
^{4b}Centre for Astroparticle Physics and Space Science (CAPSS), Kolkata, India
⁵California Polytechnic State University, San Luis Obispo, California, USA
⁶Central China Normal University, Wuhan, China
⁷Centro de Aplicaciones Tecnológicas y Desarrollo Nuclear (CEADEN), Havana, Cuba
⁸Centro de Investigación y de Estudios Avanzados (CINVESTAV), Mexico City and Mérida, Mexico
⁹Chicago State University, Chicago, Illinois, USA
¹⁰China Institute of Atomic Energy, Beijing, China
¹¹China University of Geosciences, Wuhan, China
¹²Chungbuk National University, Cheongju, Republic of Korea
¹³Comenius University Bratislava, Faculty of Mathematics, Physics and Informatics, Bratislava, Slovak Republic
¹⁴Creighton University, Omaha, Nebraska, USA
¹⁵Department of Physics, Aligarh Muslim University, Aligarh, India
¹⁶Department of Physics, Pusan National University, Pusan, Republic of Korea
¹⁷Department of Physics, Sejong University, Seoul, Republic of Korea
¹⁸Department of Physics, University of California, Berkeley, California, USA
¹⁹Department of Physics, University of Oslo, Oslo, Norway
²⁰Department of Physics and Technology, University of Bergen, Bergen, Norway
²¹Dipartimento di Fisica, Università di Pavia, Pavia, Italy
^{22a}Dipartimento di Fisica dell'Università, Cagliari, Italy
^{22b}Sezione INFN, Cagliari, Italy
^{23a}Dipartimento di Fisica dell'Università, Trieste, Italy
^{23b}Sezione INFN, Trieste, Italy
^{24a}Dipartimento di Fisica dell'Università, Turin, Italy
^{24b}Sezione INFN, Turin, Italy
^{25a}Dipartimento di Fisica e Astronomia dell'Università, Bologna, Italy
^{25b}Sezione INFN, Bologna, Italy
^{26a}Dipartimento di Fisica e Astronomia dell'Università, Catania, Italy
^{26b}Sezione INFN, Catania, Italy
^{27a}Dipartimento di Fisica e Astronomia dell'Università, Padova, Italy
^{27b}Sezione INFN, Padova, Italy
^{28a}Dipartimento di Fisica 'E.R. Caianiello' dell'Università, Salerno, Italy
^{28b}Gruppo Collegato INFN, Salerno, Italy
²⁹Dipartimento DISAT del Politecnico and Sezione INFN, Turin, Italy
³⁰Dipartimento di Scienze MIFT, Università di Messina, Messina, Italy
^{31a}Dipartimento Interateneo di Fisica 'M. Merlin', Bari, Italy
^{31b}Sezione INFN, Bari, Italy
³²European Organization for Nuclear Research (CERN), Geneva, Switzerland
³³Faculty of Electrical Engineering, Mechanical Engineering and Naval Architecture, University of Split, Split, Croatia
³⁴Faculty of Engineering and Science, Western Norway University of Applied Sciences, Bergen, Norway
³⁵Faculty of Nuclear Sciences and Physical Engineering, Czech Technical University in Prague, Prague, Czech Republic
³⁶Faculty of Physics, Sofia University, Sofia, Bulgaria
³⁷Faculty of Science, P.J. Šafárik University, Košice, Slovak Republic
³⁸Frankfurt Institute for Advanced Studies, Johann Wolfgang Goethe-Universität Frankfurt, Frankfurt, Germany
³⁹Fudan University, Shanghai, China
⁴⁰Gangneung-Wonju National University, Gangneung, Republic of Korea
⁴¹Gauhati University, Department of Physics, Guwahati, India
⁴²Helmholtz-Institut für Strahlen- und Kernphysik, Rheinische Friedrich-Wilhelms-Universität Bonn, Bonn, Germany
⁴³Helsinki Institute of Physics (HIP), Helsinki, Finland
⁴⁴High Energy Physics Group, Universidad Autónoma de Puebla, Puebla, Mexico
⁴⁵Horia Hulubei National Institute of Physics and Nuclear Engineering, Bucharest, Romania
⁴⁶HUN-REN Wigner Research Centre for Physics, Budapest, Hungary

- ⁴⁷Indian Institute of Technology Bombay (IIT), Mumbai, India
- ⁴⁸Indian Institute of Technology Indore, Indore, India
- ⁴⁹INFN, Laboratori Nazionali di Frascati, Frascati, Italy
- ⁵⁰INFN, Sezione di Bari, Bari, Italy
- ⁵¹INFN, Sezione di Bologna, Bologna, Italy
- ⁵²INFN, Sezione di Cagliari, Cagliari, Italy
- ⁵³INFN, Sezione di Catania, Catania, Italy
- ⁵⁴INFN, Sezione di Padova, Padova, Italy
- ⁵⁵INFN, Sezione di Pavia, Pavia, Italy
- ⁵⁶INFN, Sezione di Torino, Turin, Italy
- ⁵⁷INFN, Sezione di Trieste, Trieste, Italy
- ⁵⁸Inha University, Incheon, Republic of Korea
- ⁵⁹Institute for Gravitational and Subatomic Physics (GRASP), Utrecht University/Nikhef, Utrecht, Netherlands
- ⁶⁰Institute of Experimental Physics, Slovak Academy of Sciences, Košice, Slovak Republic
- ⁶¹Institute of Physics, Homi Bhabha National Institute, Bhubaneswar, India
- ⁶²Institute of Physics of the Czech Academy of Sciences, Prague, Czech Republic
- ⁶³Institute of Space Science (ISS), Bucharest, Romania
- ⁶⁴Institut für Kernphysik, Johann Wolfgang Goethe-Universität Frankfurt, Frankfurt, Germany
- ⁶⁵Instituto de Ciencias Nucleares, Universidad Nacional Autónoma de México, Mexico City, Mexico
- ⁶⁶Instituto de Física, Universidade Federal do Rio Grande do Sul (UFRGS), Porto Alegre, Brazil
- ⁶⁷Instituto de Física, Universidad Nacional Autónoma de México, Mexico City, Mexico
- ⁶⁸iThemba LABS, National Research Foundation, Somerset West, South Africa
- ⁶⁹Jeonbuk National University, Jeonju, Republic of Korea
- ⁷⁰Johann-Wolfgang-Goethe Universität Frankfurt Institut für Informatik, Fachbereich Informatik und Mathematik, Frankfurt, Germany
- ⁷¹Korea Institute of Science and Technology Information, Daejeon, Republic of Korea
- ⁷²KTO Karatay University, Konya, Turkey
- ⁷³Laboratoire de Physique Subatomique et de Cosmologie, Université Grenoble-Alpes, CNRS-IN2P3, Grenoble, France
- ⁷⁴Lawrence Berkeley National Laboratory, Berkeley, California, USA
- ⁷⁵Lund University Department of Physics, Division of Particle Physics, Lund, Sweden
- ⁷⁶Nagasaki Institute of Applied Science, Nagasaki, Japan
- ⁷⁷Nara Women's University (NWU), Nara, Japan
- ⁷⁸National and Kapodistrian University of Athens, School of Science, Department of Physics, Athens, Greece
- ⁷⁹National Centre for Nuclear Research, Warsaw, Poland
- ⁸⁰National Institute of Science Education and Research, Homi Bhabha National Institute, Jatni, India
- ⁸¹National Nuclear Research Center, Baku, Azerbaijan
- ⁸²National Research and Innovation Agency—BRIN, Jakarta, Indonesia
- ⁸³Niels Bohr Institute, University of Copenhagen, Copenhagen, Denmark
- ⁸⁴Nikhef, National institute for subatomic physics, Amsterdam, Netherlands
- ⁸⁵Nuclear Physics Group, STFC Daresbury Laboratory, Daresbury, United Kingdom
- ⁸⁶Nuclear Physics Institute of the Czech Academy of Sciences, Husinec-Řež, Czech Republic
- ⁸⁷Oak Ridge National Laboratory, Oak Ridge, Tennessee, USA
- ⁸⁸Ohio State University, Columbus, Ohio, USA
- ⁸⁹Physics department, Faculty of science, University of Zagreb, Zagreb, Croatia
- ⁹⁰Physics Department, Panjab University, Chandigarh, India
- ⁹¹Physics Department, University of Jammu, Jammu, India
- ⁹²Physics Program and International Institute for Sustainability with Knotted Chiral Meta Matter (SKCM2), Hiroshima University, Hiroshima, Japan
- ⁹³Physikalisches Institut, Eberhard-Karls-Universität Tübingen, Tübingen, Germany
- ⁹⁴Physikalisches Institut, Ruprecht-Karls-Universität Heidelberg, Heidelberg, Germany
- ⁹⁵Physik Department, Technische Universität München, Munich, Germany
- ⁹⁶Politecnico di Bari and Sezione INFN, Bari, Italy
- ⁹⁷Research Division and ExtreMe Matter Institute EMMI, GSI Helmholtzzentrum für Schwerionenforschung GmbH, Darmstadt, Germany
- ⁹⁸Saga University, Saga, Japan
- ⁹⁹Saha Institute of Nuclear Physics, Homi Bhabha National Institute, Kolkata, India
- ¹⁰⁰School of Physics and Astronomy, University of Birmingham, Birmingham, United Kingdom

- ¹⁰¹*Sección Física, Departamento de Ciencias, Pontificia Universidad Católica del Perú, Lima, Peru*
- ¹⁰²*Stefan Meyer Institut für Subatomare Physik (SMI), Vienna, Austria*
- ¹⁰³*SUBATECH, IMT Atlantique, Nantes Université, CNRS-IN2P3, Nantes, France*
- ¹⁰⁴*Sungkyunkwan University, Suwon City, Republic of Korea*
- ¹⁰⁵*Suranaree University of Technology, Nakhon Ratchasima, Thailand*
- ¹⁰⁶*Technical University of Košice, Košice, Slovak Republic*
- ¹⁰⁷*The Henryk Niewodniczanski Institute of Nuclear Physics, Polish Academy of Sciences, Cracow, Poland*
- ¹⁰⁸*The University of Texas at Austin, Austin, Texas, USA*
- ¹⁰⁹*Universidad Autónoma de Sinaloa, Culiacán, Mexico*
- ¹¹⁰*Universidade de São Paulo (USP), São Paulo, Brazil*
- ¹¹¹*Universidade Estadual de Campinas (UNICAMP), Campinas, Brazil*
- ¹¹²*Universidade Federal do ABC, Santo Andre, Brazil*
- ¹¹³*Universitatea Nationala de Stiinta si Tehnologie Politehnica Bucuresti, Bucharest, Romania*
- ¹¹⁴*University of Cape Town, Cape Town, South Africa*
- ¹¹⁵*University of Derby, Derby, United Kingdom*
- ¹¹⁶*University of Houston, Houston, Texas, USA*
- ¹¹⁷*University of Jyväskylä, Jyväskylä, Finland*
- ¹¹⁸*University of Kansas, Lawrence, Kansas, USA*
- ¹¹⁹*University of Liverpool, Liverpool, United Kingdom*
- ¹²⁰*University of Science and Technology of China, Hefei, China*
- ¹²¹*University of South-Eastern Norway, Kongsberg, Norway*
- ¹²²*University of Tennessee, Knoxville, Tennessee, USA*
- ¹²³*University of the Witwatersrand, Johannesburg, South Africa*
- ¹²⁴*University of Tokyo, Tokyo, Japan*
- ¹²⁵*University of Tsukuba, Tsukuba, Japan*
- ¹²⁶*Universität Münster, Institut für Kernphysik, Münster, Germany*
- ¹²⁷*Université Clermont Auvergne, CNRS/IN2P3, LPC, Clermont-Ferrand, France*
- ¹²⁸*Université de Lyon, CNRS/IN2P3, Institut de Physique des 2 Infinis de Lyon, Lyon, France*
- ¹²⁹*Université de Strasbourg, CNRS, IPHC UMR 7178, F-67000 Strasbourg, France, Strasbourg, France*
- ¹³⁰*Université Paris-Saclay, Centre d'Etudes de Saclay (CEA), IRFU, Département de Physique Nucléaire (DPhN), Saclay, France*
- ¹³¹*Université Paris-Saclay, CNRS/IN2P3, IJCLab, Orsay, France*
- ¹³²*Università degli Studi di Foggia, Foggia, Italy*
- ¹³³*Università del Piemonte Orientale, Vercelli, Italy*
- ¹³⁴*Università di Brescia, Brescia, Italy*
- ¹³⁵*Variable Energy Cyclotron Centre, Homi Bhabha National Institute, Kolkata, India*
- ¹³⁶*Warsaw University of Technology, Warsaw, Poland*
- ¹³⁷*Wayne State University, Detroit, Michigan, USA*
- ¹³⁸*Yale University, New Haven, Connecticut, USA*
- ¹³⁹*Yonsei University, Seoul, Republic of Korea*
- ¹⁴⁰*Zentrum für Technologie und Transfer (ZTT), Worms, Germany*
- ¹⁴¹*Affiliated with an institute covered by a cooperation agreement with CERN*
- ¹⁴²*Affiliated with an international laboratory covered by a cooperation agreement with CERN*

[†]Deceased.

[‡]Also at Max-Planck-Institut für Physik, Munich, Germany.

[§]Also at Italian National Agency for New Technologies, Energy and Sustainable Economic Development (ENEA), Bologna, Italy.

^{||}Also at Dipartimento DET del Politecnico di Torino, Turin, Italy.

[¶]Also at Yıldız Technical University, Istanbul, Türkiye.

^{**}Also at Department of Applied Physics, Aligarh Muslim University, Aligarh, India.

^{††}Also at Institute of Theoretical Physics, University of Wrocław, Poland.

^{‡‡}Also at An institution covered by a cooperation agreement with CERN.